Genetic mapping of flowering time and plant height in a maize Stiff Stalk MAGIC population

Kathryn J. Michel[*], Dayane C. Lima[*], Hope Hundley[†], Vasanth Singan[1 †], Yuko Yoshinaga[†], Chris Daum[†], Kerrie Barry[†], Karl W. Broman[‡], C. Robin Buell[2 §,**], Natalia de Leon[*,††], Shawn M. Kaeppler[*,††, §§]

[*] Department of Agronomy, University of Wisconsin – Madison, Madison, WI 53706

† U.S. Department of Energy Joint Genome Institute, Berkeley, California, 94720

‡ Departments of Biostatistics and Medical Informatics, University of Wisconsin–Madison, WI 53706

§ Department of Plant Biology, Michigan State University, East Lansing, MI 48824

** Department of Energy Great Lakes Bioenergy Research Center, Michigan State University, East Lansing, MI 48824

†† Department of Energy Great Lakes Bioenergy Research Center, University of Wisconsin – Madison, Madison, WI 53706

§§ Wisconsin Crop Innovation Center, University of Wisconsin – Madison, Middleton WI 53562

1 Ambry Genetics, 1 Enterprise, Aliso Viejo, CA - 92656

2 Center for Applied Genetic Technologies, Department of Crop and Soil Sciences, University of Georgia, Athens, GA 30602

Running Title: Maize Stiff Stalk MAGIC QTL mapping

Corresponding author:

Shawn Kaeppler
1575 Linden Dr.
Madison, WI 53706
(608) 262-9571
smkaeppl@wisc.edu

Core Ideas:

A multi-parent advanced generation intercross (MAGIC) mapping population was developed from six founder Stiff Stalk maize inbreds with commercial relevance.

Genetic mapping utilizing an update to R/qtl2 was demonstrated for flowering and plant height traits.

Genetic mapping using maize inbred and hybrid information was compared and provided insight into trait expression in inbreds relative to heterotic testcross hybrids.

Abbreviations: BSSS, Iowa Stiff Stalk Synthetic; BLUE, best linear unbiased estimator; DH, doubled haploid; ex-PVP, expired Plant Variety Protection; GWAS, genome wide association study; MAGIC, multi-parent advanced generation intercross population; PHG, Practical Haplotype Graph; PHI, Pioneer Hi-Bred, International; PVP, Plant Variety Protection; QTL, quantitative trait locus or loci; SS, Stiff Stalk

ABSTRACT

The Stiff Stalk heterotic pool is a foundation of US maize seed parent germplasm and has been heavily utilized by both public and private maize breeders since its inception in the 1930's. Flowering time and plant height are critical characteristics for both inbred parents and their test crossed hybrid progeny. To study these traits, a six parent multiparent advanced generation intercross (MAGIC) population was developed including maize inbred lines B73, B84, PHB47 (B37 type), LH145 (B14 type), PHJ40 (novel early Stiff Stalk), and NKH8431 (B73/B14 type). A set of 779 doubled haploid lines were evaluated for flowering time and plant height in two field replicates in 2016 and 2017, and a subset of 689 and 561 doubled haploid lines were crossed to two testers, respectively, and evaluated as hybrids in two locations in 2018 and 2019 using an incomplete block design. Markers were derived from a Practical Haplotype Graph built from the founder whole genome assemblies and genotype-by-sequencing and exome capture-based sequencing of the population. Genetic mapping utilizing an update to R/qtl2 revealed differing profiles of significant loci for both traits between 636 of the DH lines and two sets of 571 and 472 derived hybrids. Genomic prediction was used to test the feasibility of predicting hybrid phenotypes based on the *per se* data. Predictive abilities were highest on direct models trained using the data they would predict (0.55 to 0.63), and indirect models trained using *per se* data to predict hybrid traits had slightly lower predictive abilities (0.49 to 0.55). Overall, this finding is consistent with the overlapping and non-overlapping significant QTL found within the *per se* and hybrid populations and suggests that selections for phenology traits can be made effectively on doubled haploid lines before hybrid data is available.

INTRODUCTION

Multi-parent mapping populations are an effective tool for discovering quantitative trait loci (QTL) in plant and animal species. Multi-parent advanced generation intercross (MAGIC) populations offer a powerful QTL mapping structure because intercrossing more than two parents increases genetic diversity while managing minor allele frequency and reducing haplotype length through recombination (reviewed in Scott et al., 2020). MAGIC populations have been used to successfully dissect the genetic control of complex traits in various plant species, including Arabidopsis (Kover et al. 2009), maize (Dell'Acqua et al. 2015), rice (Ogawa et al. 2018), barley (Sannemann et al. 2015), wheat (Gardner et al. 2016), sorghum (Ongom and Ejeta 2018), tomato (Pascual et al. 2015), and cowpea (Huynh et al. 2018). Multi-parent populations balance the advantages and disadvantages of biparental mapping populations and association panels. Geneticists often rely on the cross of two individuals with contrasting phenotypes to generate a population of segregating individuals and then perform linkage analysis to associate genetic loci with the trait of interest. Recently, increased marker density due to technological advancements and rapidly declining genotyping costs allowed researchers to evaluate diverse association panels to assay historical recombination to find associations between markers and phenotypes (reviewed in Tibbs Cortes *et al.* 2021). Despite the success of these methods, both techniques face intrinsic challenges. Biparental populations rely on the genetic diversity found in just two parents, which can limit the scope of discovered QTLs to the backgrounds studied. Association panels often contain rare alleles that do not meet the minor allele frequency threshold and are discarded due to low statistical power associated with such rarity.

Thus, MAGIC populations seek to balance these characteristics by incorporating more than two genetic backgrounds while balancing minor allele frequency and increasing mapping resolution.

To study the genetic architecture of traits relevant to maize hybrid performance and adaptation, we developed a MAGIC population from six inbred lines spanning the diversity of the Stiff Stalk heterotic pool. The Stiff Stalk heterotic group was founded in the Iowa Stiff Stalk Synthetic (BSSS) breeding population, which was initiated during the 1930's by Dr. George Sprague to improve stalk quality, yield, and agronomic quality of maize inbreds (Troyer 2004). Several key inbreds were released out of BSSS, including B14 in 1953, B37 in 1958, B73 in 1972, and B84 in 1979 (Russell 1972; Russell 1979; Troyer 1999). Since their release, these founder BSSS inbreds have been used extensively by breeders in the public and private sectors in the United States, and the Stiff Stalk group has become the *de facto* source of seed parent germplasm for many hybrid breeding programs. It is estimated that B73, B14, and B37 contributed conservatively 16.4% to germplasm released by Monsanto Company, Pioneer Hi-Bred, International, and Syngenta between 2004-2008 (Mikel 2011). In a group of 1,506 lines released under Plant Variety Protection (PVP) certificates between the year 2000 and 2019, researchers found that a third of the lines had kinship estimated Stiff Stalk admixture greater than 30%, and 15% of lines had Stiff Stalk admixture greater than 50% (White et al. 2020). Thus, the Stiff Stalk heterotic group remains a vital source of commercial maize germplasm in North America. This research utilized six Stiff Stalk inbreds - B73, B84, NKH8431, LH145, PHB47, and PHJ40 – that represent key founders in commercial breeding programs. Recent work reported the genome

sequences of these inbreds (excluding B73) and found extensive genomic variation between B73 and the other five parents along with conservation of base BSSS haplotypes within each inbred (Bornowski et al. 2021).

Throughout the process of developing new inbred lines and hybrid varieties, maize breeders balance selecting for hybrid yield with other traits needed for successful inbred and hybrid seed production. Traits such as flowering time and plant height are vital to the success of an inbred within the breeding program and as a parent to a successful hybrid variety. Extensive research has been conducted on maize flowering time, including the discovery of a multitude of small to large effect QTL contributing to flowering time and photoperiod sensitivity variation in maize (Buckler et al. 2009; Xu et al. 2012; Wang et al. 2021) and the identification of several genes and regulatory elements involved in the pathway, including *ID1*, *DLF1*, *ZmCCA1*, *ZmMADS1*, *ZmCOL3*, *Vgt1*, *ZCN8*, *ZmCCT*, *ZmCCT9*, *ZmCCT10*, and *ZmMADS69* (Colasanti et al. 1998; Muszynski et al. 2006; Salvi et al. 2007; Wang et al. 2011; Hung et al. 2012; Alter et al. 2016; Jin et al. 2018; Huang et al. 2018; Guo et al. 2018; Liang et al. 2019; Stephenson et al. 2019). Flowering time and photoperiod sensitivity are determinants of maize yield because the combination leads to adaptation of maize lines to their intended environments, such that tropical lines with daylight sensitivity must undergo extensive selection for adaptation to succeed in northern regions that do not meet daylight needs of tropical plants (Xu et al. 2012). In addition, timing of flowering can influence the total length of time available for grain filling post flowering and the ability of a hybrid to mature within a frost-free seasonal interval. Within an environment, maize hybrids with full-season relative maturities often yield more than their shorter-season counterparts,

and timing of planting date to achieve flowering time before environment specific cutoffs is vital for maximizing yield potential (Baum et al. 2019). However, later-maturing varieties can face risk due to early frosts and susceptibility to seasonal drought effects (Duvick and Cassman 1999), therefore plant breeders need to carefully balance flowering time and total maturity to suit their target population of environments to maximize maize grain yield. In maize hybrid varieties, flowering time typically exhibits heterosis where the hybrid flowers sooner than the earlier of the two inbred parents, as demonstrated by a partial diallel of ex-PVP inbreds (Li et al. 2018) and an association panel of 302 diverse inbreds crossed to B73 (Flint-Garcia et al. 2009).

Like flowering time, substantial efforts have been devoted to understanding the genetic underpinnings of maize plant and ear height. Major mutations in the gibberellin and brassinosteroid pathways affecting height have been identified in addition to numerous QTL (reviewed by Salas Fernandez et al., 2009). Despite its high heritability, QTL affecting height tend to have very small effects, with the largest effect in the maize US-NAM population explaining 2.1 +- 0.9% of the variation, which suggests that maize height follows an infinitesimal model of inheritance (Peiffer et al. 2014). In addition, identification of QTL can depend on environmental conditions such as drought and nutrient stress, which may reduce the relative proportion of additive genetic variance compared to genotype by environment and error variance (Cai et al. 2012; Wallace et al. 2016). In general, taller plants can face increased root and stalk lodging pressure due to the proportionally higher placement of the ear on the stalk, which increases the ear's leverage during wind events or disease pressure. During the Green Revolution, major yield gains were made in rice and wheat by decreasing overall plant height, which

reduced the risk of lodging under more intensive agricultural management (reviewed by Khush, 2001). Maize breeders consider height selection in both inbreds and hybrids, as lodging can make harvest difficult and inefficient for both seed parents and commercial varieties. Due to heterosis, the hybrid is usually taller than the taller of the two inbred parents, as shown in a partial diallel of ex-PVP inbreds (Li et al. 2018) and in an association panel of 302 diverse lines crossed to B73 (Flint-Garcia et al. 2009).

The main objectives of this work are to: i) report a MAGIC population based on the Stiff Stalk heterotic group and its associated genetic and phenotypic resources, ii) dissect the genetic architecture of flowering time and plant height within the *per se* population of DH lines and two test cross populations, and iii) perform genomic prediction to investigate the relationship between *per se* and hybrid phenotypes.

MATERIALS AND METHODS

Population Development: Inbreds B73, B84, NKH8431, LH145, PHB47, and PHJ40 were chosen to represent the primary Stiff Stalk sub-heterotic groups (Table 1) (White et al. 2020). Biographical information for each line was obtained from the Germplasm Resource Information Network (GRIN) database (npgsweb.ars-grin.gov). The inbreds B73 and B84 were released from the BSSS in cycles five and seven, respectively, and B84 contains resistance to *Helminthosporium turcicum* (“Ht” currently known as *Setosphaeria turcica*, common name Northern Corn Leaf Blight). Inbred LH145 was developed by Holden’s Foundation Seed, Inc. (acquired by Monsanto Company in 1997) from the cross of A632Ht and CM105, both of which have B14 as a parent. Inbred NKH8431 was developed from one B73 derived line and two B14 derived lines by Northrup, King & Company. Inbreds PHB47 and PHJ40 were both released by Pioneer

Hi-Bred, International (PHI). Inbred PHB47 was made from a cross between B37 and SD105, with two backcrosses to B37 before inbred development. Inbred PHJ40 is an early flowering flint and Stiff Stalk line developed in Ontario, Canada, with previously demonstrated admixture with B37 (White et al., 2020). All inbred lines except B73 previously underwent whole genome, reference guided assembly, which revealed extensive genetic and genomic diversity between the five lines and B73 (Bornowski et al. 2021).

Table 1. Origins of Stiff Stalk inbred lines

Line	**Originator**	**Sub-heterotic group**	**PI number**
B73	Iowa State University	B73	PI 550473
B84	Iowa State University	B73	PI 608767
LH145	Holden's Foundation Seed, Inc.	B14	PI 600959
NKH8431 (alias H8431, NPH8431)	Northrup, King & Company	B14	PI 601610
PHB47 (alias B47)	Pioneer Hi-Bred International, Inc.	B37	PI 601009
PHJ40	Pioneer Hi-Bred International, Inc.	Flint	PI 601321

Table 1 Sub-heterotic groupings from White et al., 2020

The population, named WI-SS-MAGIC, was initiated at the University of Wisconsin during summer 2008. The six parents were crossed in a half diallel. Next, every possible

F_1 hybrid combination cross was attempted, and seed was included in the subsequent balanced bulk to maintain equal representation of all parents and account for any failed crosses. In subsequent generations, plants from the population bulk were randomly intermated by designating each plant as a pollen parent or seed parent and using the individual only once for crossing. Balanced bulks were made after harvest of the first intermating and a subset of the population (hereafter “Subset A”) was sent for doubled haploid (DH) induction, provided as in-kind support by AgReliant Genetics. The remaining balanced bulk was randomly intermated for two additional generations and then sent for DH induction (hereafter “Subset B”). Individuals in Subset A were given coded names beginning with W10004 and numbered from 1 to N, where N is the number of individuals (i.e. W10004_0001 through W10004_04xx), and individuals in Subset B were named using W10004 and a number from 500 to 500+N, where N is the number of individuals returned (i.e. W10004_0500 through W10004_xxxx) (Table S1).

Collection of *Per Se* DH Line Phenotypic Data: A set of 779 DH lines was planted during summers 2016 and 2017 at the West Madison Agricultural Research Station in Verona, WI (Table S1). Subset A and Subset B groups were organized as subblocks within a randomized complete block (RCB) design with two replications. Parents were included as checks in both subblocks. Both trials were planted in fields that followed soybeans in the previous year and were managed with standard agronomic practices. Detailed information about planting dates and densities, soil types, and nutrient and pesticide management is presented in Supplemental Table 2. Three representative plants per plot were measured for plant and ear height. Plant height was measured as the height from the ground, in centimeters, to the collar of the flag leaf, while ear height

was the height, in centimeters, from the ground to the base of the node subtending the uppermost ear. Growing degree units to anthesis and silking were measured on a whole plot basis (AnthGDU and SilkGDU, respectively). Anthesis and silking were measured as the number of days from planting it took to observe approximately 50% of the plants in the plot to reach pollen shed and silk extrusion, respectively. Dates were converted to growing degree units using a base temperature of 50º F and maximum temperature of 86º F (Pope 2008) using temperature data obtained from the weather station located at the University of Wisconsin (UW) West Madison Agricultural Research Station to standardize for differential daily heat unit accumulation across years. Since lines developed through doubled haploidy are expected to be genetically uniform, lines with observable phenotypic segregation were discarded. Severely lodged plants were not evaluated for height characteristics. To remove outlier data points, individual plant measurements were discarded if the ear height to plant height measurement ratio was less than 0.25 or greater than 0.75, and whole plot ear or plant height measurements were discarded if the within plot variance was greater than 500 cm^2.

Generation of Hybrids and Collection of Phenotypic Data: Hybrid seed was produced by crossing the WI-SS-MAGIC population to PHJ89 and DKH3IIH6 (hereafter 3IIH6). The hybrid populations were named SS-PHJ89 and SS-3IIH6. PHJ89 is an Oh43-type inbred line developed by Pioneer Hi-Bred (White et al. 2020). The inbred 3IIH6 is an Iodent-type inbred line developed by DeKalb Genetics Corporation (acquired by Monsanto in 1998, now owned by Bayer AG) through selfing the F_1 Hybrid PHI3737 (Dekalb Plant Genetics 1994). PHJ89 and 3IIH6 are related by pedigree through their founder PHG47, which is one of the two parents of PHJ89 and one of the parents of

hybrid variety PH3737 from which 3IIH6 was generated through selfing, so they are expected to contain regions of identity by descent (Pioneer Hi-Bred International Inc. 1992; Mikel 2011). Hybrids were grown during summers 2018 and 2019 at the UW West Madison Agricultural Research Station in Verona, Wisconsin and at the UW Arlington Research Station in Arlington, WI. Hybrids were blocked by tester, and each block included at least five replicates each of two commercial hybrids (DKC50-08RIB and DKC54-38RIB) and two replicates of each respective population parent-tester combination, when seed was available. All trials were incompletely replicated, where each hybrid genotype was grown at least once in each experiment with a consistent random subset replicated a second time. A total of 689 SS-3IIH6 hybrids were grown, of which 316 were replicated, while a total of 561 SS-PHJ89 hybrids were grown, of which 377 were replicated (Table S1). The same set of replicated and unreplicated lines were grown across years and locations, with unique plot randomizations for each year-location combination. Replicated hybrids were randomized among the unreplicated hybrids within their respective tester blocks. All trials were planted in fields that followed soybeans in the previous year and were managed with standard agronomic practices. Detailed information about planting dates and densities, soil types, and nutrient and pesticide management is presented in Table S2. Flowering time growing degree units were recorded in the same manner as previously described for the *per se* population using weather data obtained from each research station. Flowering time was recorded for all hybrid plots in West Madison and for approximately 36% and 33% percent of hybrid plots in Arlington in 2018 and 2019, respectively. Plant height and ear height were measured on three competitive plants per plot for all plots. Stand counts were

recorded manually, and plots were discarded if they contained fewer than twenty plants. The 2019 West Madison trial experienced extremely wet and cold germination conditions, which led to low stand counts for the SS-3IIH6 block. Only 19% and 38% of the plots had stands greater than 50 and 40 plants, respectively, which prompted us to discard the height data due to inconsistent interplant competition but keep flowering time data due to good correlations with flowering time from the previous year. To remove outlier data points, individual plant measurements were discarded if the ear height to plant height measurement ratio was less than 0.25 or greater than 0.75, and whole plot height measurements were discarded if the within plot variance was greater than 500 cm^2. Plot average height measurements and flowering GDU measurements that were more than three standard deviations away from the experiment wide mean were discarded.

Analysis of Phenotypic Data: A two stage approach was taken to analyze plot mean phenotypic data (Table S3). In stage one, following the procedures of (Rogers et al. 2021), linear mixed models were fit using R/ASReml version four (Butler et al. 2017; RCoreTeam 2018) for each population within each environment using genotype as a fixed effect and replicate as a random effect. Next, models were fit with all combinations of autoregressive first order (AR1) and IID residual covariance structures of the x and y grid coordinates of the plot locations to account for spatial variation. The model with the lowest Schwarz's Bayesian Information Criterion (BIC) (Schwarz 1978) was chosen to represent the environment, and the BLUEs and standard errors were extracted from the model (Table S4). Due to our incomplete block structure, the residual spatial correlations were restricted to $-0.6 < r < 0.6$. Any models with correlation outside this

range were reset to using no residual covariance structure. In stage two, genotypes were fit as fixed effects and environment and genotype by environment interaction terms were set as random effects. To weight the second stage analysis, the reciprocals of the first stage BLUE standard errors were carried forward, which represent the genotype by replication interactions, and the units variance was constrained to one. Within each experiment, any phenotypic BLUE that fell outside 2.5 times the interquartile range (IQR) was discarded as an outlier. Following the data cleaning described in the previous sections and the *post hoc* cleaning based on IQR, BLUEs were calculated for 730 DH lines, 658 SS-3IIH6 hybrids, and 535 SS-PHJ89 hybrids. Parental check lines were included in the analysis because they constitute the same population as the experimental lines, while commercial check hybrids were not included in the analysis. To estimate variance components and calculate heritability, the same model was used except genotype was set as a random effect. Heritability was calculated as follows (Cullis et al. 2006):

[1] $h^2_{Cullis} = 1 - PEV/2\sigma^2_g$

using the prediction error variance (PEV) and genetic variance ($\hat{\sigma}^2_g$) obtained from the stage two analysis. To compare phenotypic variances across populations, the squared coefficient of variation was calculated to correct for the differences in scale between *per se* and hybrid phenotypes (Falconer and Mackay 1989). Pearson correlations within and between phenotypes were calculated on trait BLUE values within and between the DH and two hybrid populations.

Genetic Data

Sequencing Using Exome Capture: Exome capture sequencing was performed on 701 DH lines from the WI-SS-MAGIC (Table S1) using a custom capture design acquired from Roche Diagnostics Corporation (Indianapolis, IN). Probes were designed to target the 5' and 3' ends of the untranslated regions (UTRs) of the maize B73_RefGen_v2 genic regions and presence absence variation (PAV) regions derived from alignment of whole genome sequencing reads of a core set of 32 inbreds to B73 (Brohammer et al. 2018; Mazaheri et al. 2019). In total, 82,351 genic regions (approximately 26.5 Mb) and 492 PAV regions (approximately 2.8 Mb) of the maize genome were targeted using tiled, variable length probes, with an average probe size of 75 nt (File S1). Any overlapping regions were collapsed into a single target. The target regions ranged in size from 50 to 49,777 nucleotides (nt), with a mean size of 353.6 nt (File S2). Briefly, DNA was extracted using seedling tissue using a modified CTAB method (Saghai-Maroof et al. 1984), sheared, and hybridized with adapters prior to SeqCap EZ solution capture, as previously described (Mascher et al. 2013) (File S3). DNA was then amplified, enrichment quality control performed, and libraries sequenced by the United States Department of Energy Joint Genome Institute (JGI) in paired end mode on the Illumina HiSeq 2500. Raw sequence quality was evaluated using FastQC v0.11.5 (https://www.bioinformatics.babraham.ac.uk/projects/fastqc) and MultiQC v1.0 (Ewels et al. 2016). Reads were then trimmed, low quality bases removed, and adapters removed using Cutadapt v1.14 (Martin 2011) with the following parameters: --length 150, -m 20, -q 20, 20, --times 2, and -g/-a/-G/-A along with their respective adapter sequences. After cleaning, read quality and adapter content were evaluated again using FastQC v.0.11.5 and MultiQC v1.0.

Genotyping By Sequencing: Additional genotyping was performed on 144 DH lines using Genotyping-by-Sequencing (GBS) at the University of Wisconsin Biotechnology Center (Table S1). Briefly, dual digest GBS was performed with restriction enzymes *Pst*I and *Msp*I on frozen seedling leaf tissue (Elshire et al. 2011; Poland et al. 2012). DNA was sequenced using an Illumina NovaSeq6000 in paired end mode 150 nt and analyzed using bcl2fastq v2.20.0.422 (San Diego, CA, USA). Read one was demultiplexed and barcodes were removed using Tassel-5-Standalone plugin "ConvertOldFastqToModernFormatPlugin" with parameters "-e PstI-MspI" and "-p R1" (Bradbury et al. 2007). Read two was not included in future analysis.

Practical Haplotype Graph: A Practical Haplotype Graph (version 0.0.30) was built using B73 v5 as the reference (Bradbury *et al.* 2021, maizegdb.org). The B73 RefGen_v5 annotation of genes (Zm-B73-REFERENCE-NAM-5.0_Zm00001eb.1.gff3, available at maizegdb.org) was used to make the initial reference ranges, which were supplied to the "CreateValidIntervalsFilePlugin" to collapse any overlapping ranges and format for input into PHG. B73 RefGen_v5 was loaded as the reference assembly using the "MakeInitialPHGDBPipelinePlugin", followed by the other five parental *de novo* genome assemblies using the "AssemblyHaplotypesMultiThreadPlugin" (Bornowski et al. 2021). The "AssemblyHaplotypesMultiThreadPlugin" uses mummer4 to align each assembly to the reference by chromosome in parallel (Marçais et al. 2018). Next, B73 was added to the graph using the "AddRefRangeAsAssemblyPlugin" which allows B73 haplotypes to be included as potential parental sequences.

A ranking file was generated by counting the number of haplotypes found within each assembly. The ranking file is necessary when two or more haplotypes are collapsed into

a consensus haplotype, where the sequence of the highest-ranking line will represent the group. Consensus haplotypes were made using the PHG shell script "CreateConsensi.sh" with parameters "mxDiv=0.0001" and "minTaxa=1". All other parameters were left as default. The value of "mxDiv=0.0001" was chosen such that genic regions would only be collapsed if they were truly identical, since over 90% of maize gene models are shorter than 10,000 bp. After consensus haplotypes were generated, the "ImputePipelinePlugin" with parameter "-imputeTarget pathToVCF" was used to index the pangenome, map exome capture and GBS reads to the graph, use a Hidden Markov Model to find paths through the graph for each taxon, and call SNPs in the genic reference regions for the progeny population. Exome capture reads were aligned as paired end sequences, while the GBS reads were aligned as single end sequences. Parental assembly genic SNPs were extracted from the graph using the "FilterGraphPlugin" and "PathsToVCFPlugin". Due to the expected homozygosity of the DH lines and parental assemblies, only homozygous SNPs were generated from the PHG.

Markers were filtered and selected for mapping using Tassel-5-Standalone (Bradbury et al. 2007). The combined file of parental and population individuals (File S4) was filtered to remove any non-Stiff Stalk individuals that were included as checks, SNPs with any missing parental data were removed, minor SNP states were set to missing to remove third, fourth and other alleles, and the SNP was removed if the minor allele frequency was less than 0.05. To reduce correlation between SNPs and decrease QTL mapping computational time, 100,000 evenly spaced SNPs were selected across the ten chromosomes and converted to numerical major or minor alleles.

Population genetic characteristics: Multidimensional scaling (MDS) was performed using 1.8 million unfiltered genic SNPs to confirm lack of population structure. A distance matrix was calculated using the "DistanceMatrixPlugin" from Tassel-5-Standalone with default parameters (Bradbury et al. 2007). In R, cmdscale() was used to calculate classical MDS on the distance matrix for the first two dimensions (RCoreTeam 2018). Allele frequencies were calculated on the set of 100,000 SNPs used for QTL mapping.

QTL Mapping: Quality control analyses, single-marker QTL mapping, and SNP associations were performed using R/qtl2 with the cross-type corresponding to our mating design, "dh6" (Broman et al. 2019). Whenever individuals underwent both exome capture and GBS, the GBS reads were used to generate markers for QTL mapping. To prepare the data, a control file was created using the function write_control_file() from R/qtl2, which specifies the cross type for our population, the file names of the population and parental SNPs, the physical map coordinates for the SNPs, the phenotype file, the cross information file, which contains the number of meiosis used to generate each individual, and the parental alleles "AA" through "FF". Due to the high density of markers, a genetic map was approximated by converting each SNP's megabase pair position to centiMorgans using the B73 RefGen_v5 chromosomal genome length of 2132 Mbp divided by the composite US-NAM genetic map length of 1456.68 cM (Li et al. 2015). The control file and all materials needed for mapping are provided as Supplemental File S5.

Any line with segregating *per se* phenotypes had previously been removed from further analysis. To identify potential sample duplicates, the function compare_geno() was used

to calculate marker matching for all pairwise comparisons, and any pair of individuals with greater than 95% marker sharing was removed. Conditional genotype probabilities, or the true genotype underlying the observed markers, were calculated using a Hidden Markov Model (HMM) in the function calc_genoprob(), with an error probability of 0.01. (Broman and Sen 2009, Appendix D). After calculating genotype probabilities, the maximum marginal probability of the parental haplotypes was calculated and the total number of crossover events per individual was identified using the function count_xo(). Crossover locations were estimated using the function locate_xo(). Lines with unusually high numbers of total crossovers could be the result of sample contamination during population development or maintenance, as the HMM cannot accurately deduce the correct underlying parental haplotypes in non-parental regions, and instead frequently switches back and forth among the parent haplotypes. Lines in Subset A with more than 150 crossovers or lines in Subset B with more than 250 crossovers were removed from further analysis.

After quality control, 657 individuals remained with phenotypes and genotypes for mapping purposes (Table S1). The genotype probabilities were used to calculate a kinship matrix, so the analysis could account for the relatedness between individuals using the “leave one chromosome out” (LOCO) method, which uses a kinship matrix derived from all other chromosomes except the chromosome under study to allow for a random polygenic effect (Yang et al. 2014). Next, single marker analysis was performed using a linear mixed model with the kinship matrix as a covariate to find associations between genotype and phenotype. Log of odds (LOD) thresholds were determined as the 95th percentile LOD score after 1,000 permutations of the founder probabilities

using the function scan1perm() (Churchill and Doerge 1994; Cheng and Palmer 2013). Bayesian credible intervals for QTL peaks were calculated using the function find_peaks(), with LOD thresholds specific to each phenotype and probability of 0.95. To declare two QTL under one large peak, the LOD threshold was required to drop by at least five. Chromosome-wide QTL BLUP effects were calculated using the function scan1blup(), and single locus BLUP effects were estimated using fit1() with “blup=T”.

In addition to single marker QTL mapping, we also performed SNP association using the R/qtl2 function scan1snps(), with the same kinship matrix as previously described provided to account for population structure. Finally, not all DH lines included in the *per se* mapping were used to make the hybrid populations. To account for this difference in sampling between the *per se* traits and the hybrid traits, the sets of DH lines included in each hybrid population were used to repeat the mapping and permutation procedures for each *per se* trait that corresponded to a hybrid trait.

Genomic Prediction: To test the correlation between *per se* and hybrid phenotype based on the DH population *per se* genetics, we performed genomic prediction using the 100,000 SNP markers used for QTL mapping. We used the package R/rrBLUP to perform ridge regression on the marker effects, which is equivalent to calculating genomic estimated breeding values using a realized relationship matrix (Hayes et al. 2009; Endelman 2011). We used fivefold cross validation to train and test the models predicting *per se* and hybrid traits. We partitioned the phenotypic data into five segments and used four segments for training the model and the remaining portion for testing the model. We predicted the phenotypes for each of the five testing segments and calculated the correlation between the predicted and observed phenotypes, which

comprised one replication. We repeated this process 100 times for each of the phenotypes. To indirectly predict the hybrid phenotypes from the parental *per se* phenotypes, we calculated the correlation between the testing set predicted *per se* phenotypes and the observed hybrid phenotypes.

RESULTS

Phenotypic variation: Plant height and AnthGDU in the *per se* and hybrid populations showed normal distributions, and heritability ranged from 0.83 for SS-3IIH6 AnthGDU to 0.89 for SS-PHJ89 AnthGDU (Figure 1, Table S5). The genetic variance for *per se*, SS-3IIH6, and SS-PHJ89 AnthGDU was 2781.6 GDU^2, 1148.6 GDU^2, and 944.3 GDU^2, respectively, while the genetic variance for *per se*, SS-3IIH6, and SS-PHJ89 plant height was 386.3 cm^2, 150.1 cm^2, and 144.6 cm^2, respectively. Similarly, the squared coefficient of variation for *per se*, SS-3IIH6, and SS-PHJ89 AnthGDU was 18.00, 9.24, and 7.33, while the squared coefficient of variation for *per se*, SS-3IIH6, and SS-PHJ89 PH was 124.93, 26.79, and 22.35, respectively. All traits except *per se* and SS-PHJ89 AnthGDU exhibit transgressive segregation, where one or more progeny DH lines have more extreme values than all the parents (Figure 1). The parental line PHJ40 was the earliest flowering individual in the *per se* and SS-PHJ89 experiment.

Anthesis and silking are highly correlated within both DH lines and hybrids, ranging between Pearson r=0.83 for *per se* SilkGDU to *per se* AnthGDU to r=0.93 for SS-3IIH6 SilkGDU to AnthGDU (data not shown). The correlations between *per se* AnthGDU and SS-3IIH6 AnthGDU is r=0.64 and *per se* AnthGDU to SS-PHJ89 AnthGDU is r= 0.66 (Figure 2A and 2B). Correlation between AnthGDU for the two hybrid populations is higher at r=0.69 (Figure 2C). Plant height and ear height are also highly correlated

within DH lines and hybrids. Correlations between plant height and ear height are r=0.79 within both the *per se* and SS-3IIH6 populations and r=0.83 within the SS-PHJ89 population (data not shown). *Per se* to hybrid plant height correlations are r=0.64 between DH lines and SS-3IIH6 and r=0.71 between DH lines and SS- PHJ89 (Figure 2D and 2E). Hybrid to hybrid plant height correlation is 0.72 (Figure 2F). The high correlation between hybrids is expected, due to both the highly additive nature of flowering time and height and the relatedness between testers 3IIH6 and PHJ89.

On average, the SS-3IIH6 population is 71.5 cm taller and sheds pollen 90.2 GDU earlier than its DH counterparts, and the SS-PHJ89 population is 82.0 cm taller and sheds pollen 101.1 GDU earlier than its DH founders. Finally, height and flowering are also correlated within populations, where r=0.35, 0.41, and 0.59 for the *per se,* SS-3IIH6, and SS-PHJ89 populations, respectively (Figure S1).

Practical Haplotype Graph: The 39,035 B73 RefGen_v5 annotated gene models were used as initial reference ranges, and after collapsing overlapping ranges, 36,399 genic ranges remained, and 36,401 intergenic ranges were inserted between genic ranges for a total of 72,800 ranges. The average genic range width was 4755 bp, while the average intergenic range width was 53,811 bp. The theoretical maximum number of haplotypes per reference range is six, which represents either all inbreds having sequence that aligns to the reference (including reference to reference alignment), or five inbreds that have alignment with the reference and one with a missing haplotype. Not all assemblies have sequence that aligns to every range owing to structural variation between the parental genomes. Each parental assembly had different numbers of total haplotypes aligning to B73, from 51,070 haplotypes for PHJ40 to

66,890 for B84. PHJ40 is known to be more structurally diverse from the other founders (Bornowski et al. 2021), and the next lowest number of aligned haplotypes was 62,144 for LH145. After collapsing haplotypes into consensus sequences, the average number of haplotypes per PHG reference range was reduced from 5.7 to 3.3 (Figure 3A). Identity by descent relationships are present between all of the lines due to their common heritage from the BSSS, and these relationships are strongest between B73 and B84, B73 and NKH8431, and NKH8431 and LH145. Consensus parental and population haplotype identification numbers are presented in Table S6.

Population genetic characteristics: Multidimensional scaling (MDS) confirmed the lack of population structure within our population (Figure 3B). The parental inbred lines fall on the perimeter of the point cloud, with no discernable clustering of progeny individuals. Allele frequency distributions for the major and minor alleles appear as expected, with peaks near 1/6 and 2/6, corresponding to private and two-way sharing of alleles within the parents, respectively (Figure 3C). The founder probabilities and the total number of observable crossovers were calculated using R/qtl2. The two population subsets have overlapping distributions for the total number of crossovers per individual. While examining the locations and total numbers of crossovers present within individuals, we found some areas of the genome in certain individuals contained unusually high numbers of crossovers. Such areas indicate that the Hidden Markov Model fails to choose a single founder for the area, and instead rapidly switches between founders. While some individuals had high total genome wide incidence of crossovers, which indicates a sample mix-up, some lines had isolated areas of high crossover in only a few regions. Small areas of high crossover could be caused by

several factors, including residual heterozygosity in the founder inbreds, introgression from the DH inducer (Li et al. 2009), contamination during population development from an inbred closely related to one of the founders, or technical issues during the SNP calling pipeline. In addition, using a PHG with imputation to generate SNPs for the population forces each individual to have haplotypes only from the population founders which complicates identifying areas of inducer introgression or contamination. Most importantly, QTL mapping results did not change significantly between the raw, full set of lines and the cleaned, reduced set of lines filtered for high total crossovers (150 crossovers for Subset A, 250 crossovers for Subset B), indicating that our results are robust to this low level of uncertainty.

After removing individuals with high numbers of total crossovers, the Subset A (three total meioses to generate DH lines) has an average of 60 crossovers, while Subset B (five total meioses to generate DH lines) has an average of 101 crossovers (Figure 3D). The parental haplotypes for a set of eight population individuals reveal a mosaic of the founder genotypes (Figure S2). The top row of individuals belongs to the Subset A and show longer parental haplotypes than the bottom row of individuals, which belong to Subset B. In many individuals, there are chromosome sections plotted in white, which correspond to areas where the founder probabilities do not rise above 0.5. This is expected, due to the related nature of the population founders and the segments of identity by descent between them. For example, large stretches of identity by descent between B73 and B84 due to their selection out of the BSSS would make assigning population haplotypes to either of the parents difficult, and this issue is compounded by the presence of BSSS lines in the pedigrees of the other population parents. After

removing individuals with high crossovers, some regions of local high crossover frequency remain, potentially due to introgression from the DH inducer which has been previously observed (Li et al. 2009) or possible factors such as residual heterozygosity in founder inbreds.

QTL Mapping

QTL Mapping and SNP Association: To analyze flowering time and plant height, we took both a linkage mapping and SNP association approach. Linkage mapping relies on linear regression of the phenotypes on the matrix of founder probabilities, while SNP association regresses the phenotypes on the biallelic marker states. We found high concordance between linkage mapping and association analysis, where the most significant loci were identified for all traits by both approaches (Figures S3 and S4). Thus, we will refer to the linkage mapping results to represent our findings.

Flowering Time: Mapping for AnthGDU revealed several significant peaks across the ten chromosomes in the WI-SS-MAGIC DH population (Figure 4A, Figure S5). The most significant peaks appear on chromosome three at 156.3 and 163.1 Mbp and chromosome eight at 127.9 Mbp (Table S7). Peaks for anthesis and silking highly colocalized, which is expected due to the high correlation of the phenotypic values at r=0.83 (Figure S3). Several of the significant loci are near the location of other known flowering time genes. For example, chromosome three contains *ZmMADS69*, also known as *Zmm22*, and chromosome eight contains *ZmRap2.7* and *ZCN8*, as noted on Figure 4A. All three genes are known to regulate flowering time (Guo et al. 2018; Liang et al. 2019). Despite the high correlations between *per se* and hybrid flowering, several QTL that are significant in the *per se* population lose their significance in one or both

hybrid populations. The large peak on chromosome eight containing *ZmRap2.7* and *ZCN8* is not significant in the SS-PHJ89 population, despite retaining its significance in the group of DH lines used to make the hybrid population (Figure 4C). The same locus remains significant in the SS-3IIH6 population, albeit with a smaller LOD score (Figure 4B). Loss of significance indicates a loss in variation, such that the tester may have a dominant allele that masks the variation within the DH population. This suggests that there are contrasting loci present between the two testers, where PHJ89 has a dominant locus relative to the *per se* population while 3IIH6 does not.

We calculated BLUP QTL effects for *per se* AnthGDU on chromosomes three and eight and found allelic series at the significant loci on both chromosomes (Figure 5). On chromosome three, PHB47 provides the early flowering allele and LH145 provides the late flowering allele, while on chromosome eight PHJ40 provides the early allele, and B73 and B84 provide later alleles. It is notable that LH145 is the second earliest parent of the population and PHB47 flowers near the mean of the population, demonstrating that alleles for early and late flowering segregate within the parents. Using a single QTL model to fit the BLUP effects for the chromosome three peak at 163,105,981 bp, the most extreme alleles from the parents show a -27.2 +/- 8.8 GDU effect for PHB47 and +22.6 +/- 8.9 GDU effect for LH145. For the peak on chromosome eight at 127,898,534 bp, the most extreme effects are -24.5 +/- 8.9 GDU from PHJ40 and +17.1 +/- 8.9 GDU from B73.

Plant Height: Like flowering time, many significant peaks were also found for plant and ear height, such as on chromosomes one, two, three, and ten (Figure 6A, Figure S5, and Table S7). The most significant locus on chromosome one is located at 225.4 Mbp

and it contains *brd1*, a gene which is involved in the brassinosteroid pathway and for which a mutant allele causes severe dwarfism (Makarevitch et al. 2012). Likewise, the most significant locus on chromosome three at 8.9 Mbp contains another gene discovered through mutational studies, *DWARF1* (*d1*), which is involved in the gibberellin pathway (Chen et al. 2014). Fewer loci colocalized for plant and ear height compared to AnthGDU and SilkGDU (Figure S4). Most interestingly, a peak on chromosome six at 105.8 Mbp appears for plant height in the SS-3IIH6 population, but not in the SS-PHJ89 population (Figure 5B). This peak is near *ubi3*, previously found to be associated with height traits (Ding et al. 2016). Previous studies have identified an epistatic interaction between *ubi3* and *br2* (Xiao et al. 2021), so we investigated the parental effects of the peak on chromosome six at 105,826,214 bp for both hybrid populations and found that the LH145 allele had an effect of +3.5 +/- 1.7 cm, while the B73 allele had an effect of -4.7 +/- 2.0 cm in the SS-3IIH6 population (Figure S6). Here again, *per se* B73 is the tallest of the parents while *per se* LH145 is the second shortest and their allelic effects are opposite of their overall phenotypes, but their hybrid phenotypes are both closer to the population mean. For comparison, the insignificant chromosome six locus in the *per se* and SS-PHJ89 populations shows no such differentiation between the parents (Figure S5). The genetic variance for plant height in the SS-3IIH6 population was 151.1 cm^2, so the allelic effects here are a small proportion of the total variance.

Genomic Prediction: Because information on the DH lines was available before hybrid test crosses were made, we tested the predictive abilities of several direct and indirect genomic prediction models (Figure 7). As expected, the most successful models were

those that were trained on the data that was most directly related to the predicted set, such as prediction within the hybrid SS-PHJ89 set and within the SS-3IIH6 set for plant height (r=0.63 and r=0.60, respectively) and prediction within the *per se* set for anthesis (r=0.61). Predictive abilities between test cross populations were moderate, with AnthGDU predictive abilities for SS-3IIH6 to SS-PHJ89 and vice versa of r=0.55 and 0.54, and plant height at 0.57 and 0.53, respectively. The correlations of the indirect predictions of *per se* to hybrid phenotypes were lower, but still greater than r=0.48. It is important to note that correlations do not consider the difference in scale between the *per se* and hybrid populations and cannot account for the population mean heterotic effect on both flowering time and plant height between the populations. Finally, we wanted to test the feasibility of using predicted *per se* data to discard DH lines from our breeding program that either are too tall or flower too late for our environment. We compared the predicted *per se* AnthGDU and *per se* plant height values to their observed values, and colored DH lines based on their status in the top 15th percentile for either the predicted or observed value (Figure S7). We maintained this color scheme when plotting the DH line's observed hybrid values to assess the combination of genomic prediction ability and tester response. Overall, we found that the DH lines in the top 15th percentile for the predicted trait but not for the observed trait tended to be the DH lines that would make hybrids that are satisfactory to our breeding program's needs, while DH lines that were in the top 15th percentile of observed values tended to have higher hybrid values. These results are expected, especially considering the high correlations between *per se* and hybrid phenotypes and the lower predictive ability of the *per se* to hybrid models.

DISCUSSION

QTL mapping in multi-parent populations: Several multi-parent populations have been developed in maize, including MAGIC populations from Italy and Spain (Dell'Acqua et al. 2015; Jiménez-Galindo et al. 2019), four-parent populations from China and the US (Ding et al. 2015; Mahan et al. 2018), and nested association mapping populations from the US, China, and Europe (Yu et al. 2008; Li et al. 2013; Bauer et al. 2013; Giraud et al. 2017). The existing MAGIC, US-NAM, and CN-NAM populations use a variety of inbreds that sample the diversity of maize genetics, and the European NAM populations focus on the Dent and Flint heterotic groups in addition to factorial crosses made between recombinant inbred lines. Our population concentrates the founders within the Stiff Stalk heterotic group. An advantage to focusing on the Stiff Stalk group is that maize breeding relies on recycling genetics within heterotic groups to make new parents and crossing parents between groups to make hybrids. In a factorial mating design between Flint and Dent multiparent populations, it was discovered that the majority of general combining ability QTL were specific to one heterotic group (Giraud et al. 2017; Seye et al. 2019). Thus, blending the genomes of parents within a single heterotic group versus across the diversity of maize creates a more applicable population to study the subset of alleles present within Stiff Stalk seed parent germplasm released in North America. Breeding based on heterotic groups is expected to drive diverging allele frequencies between groups and constraining our mapping population to a single heterotic group allows us to examine the effects of these alleles on agronomic and yield related traits within their intended context. Mixing multiple founders takes advantage of historical recombination in addition to recombination

introduced through population development. Multiple founders within a single population allows the study of allelic series at loci of interest, such as for AnthGDU on chromosomes eight and three (Figure 5).

QTL mapping in the WI-SS-MAGIC: Large efforts have been made by the plant research community to elucidate the control of complex traits such as flowering time and height. Our results confirm the previous findings of numerous authors, especially the candidate genes highlighted in Figures 4 and 6. Similar loci were found within the *per se* and hybrid populations, but there was variation between the populations, indicating that non-additive variation impacts the hybrid phenotypes (Supplemental Figure 5). For flowering time, the loss of significance of the QTL on chromosome eight indicates the PHJ89 tester has a completely dominant locus compared to the *per se* population and compared to the other tester, 3IIH6. Our results demonstrate that QTL detection depends on the genetics of the tester when mapping in hybrid populations. While it is possible that the absence of a signal in the hybrid population could be due to environmental or genotype by environment effects, the high heritabilities support the large role of genetic variation.

For plant height, a significant locus exists within the hybrid SS-3IIH6 population that is absent in the *per se* population, which could indicate an epistatic interaction between the tester and population genotypes. This locus has been previously described in the context of both inbred and hybrid populations (Ding et al. 2016; Xiao et al. 2021). Ding et al. (2016), used a near isogenic line from the US-NAM family B73 × Tzi8 crossed to B73 to finemap the QTL to 95-96 Mbp on chromosome six. Like our study, Xiao et al. (2021), found a plant height QTL near 95.8 Mbp on chromosome six within one test

673 cross population but not in the inbred population, and provides a schematic outlining the
674 epistatic derepression uncovered by this locus. In theory, there is the potential to study
675 epistasis between more than two founders within a MAGIC population. For the WI-SS-
676 MAGIC population, comparing the founder states for two loci results in 36 total digenic
677 classes. We separated our population into these classes for the two most significant loci
678 for *per se* AnthGDU and found the mean number of individuals per class was 16.5, with
679 a range of seven to 44 individuals (Supplementary Figure 8). Smaller population size in
680 some of the sets exacerbates this issue of power. We repeated the procedure for the
681 SS-3IIH6 plant height loci on chromosome one and six and found a mean of 11.0
682 individuals per class, with a range of zero to 27, and nine classes have fewer than five
683 observed individuals (Supplementary Figure 9). The limited number of observations per
684 digenic class restricts the ability to statistically evaluate interaction between loci.

685 **QTL mapping in DH lines and hybrids:** Previous work in mapping QTL across testers
686 has found high concordance between plant height QTL discovered in different test cross
687 populations and minimal digenic epistasis, despite evidence for epistasis under
688 generation means analysis (Lübberstedt et al. 1997; Melchinger et al. 1998). Tester
689 relatedness also influences the ability to discover QTL, where a tester unrelated to the
690 population uncovers QTL for additive traits more effectively than related testers
691 (Frascaroli et al. 2009). Another study of a biparental RIL population crossed to four
692 testers found that mapping the mean test cross height was sufficient to identify shared
693 loci between testers (Austin et al. 2001). Recent work by Xiao et al. (2021), examining
694 heterosis for over 42,000 hybrids generated by crossing 1428 multi-parent lines with 30
695 testers found that epistasis plays a role in generating heterosis, contradicting previous

work demonstrating the low impact of epistasis (Hinze and Lamkey 2003; Mihaljevic et al. 2005).

We documented our population's response to two testers to better understand the heterotic effect of Iodent (3IIH6) and Oh43 (PHJ89) type testers on the WI-SS-MAGIC population. Understanding *per se* phenotypes requires mapping in an inbred population, while understanding an inbred's response to a tester requires evaluating and mapping traits in the hybrid population. We found the hybrid populations to have less than half the variation of the *per se* population, which could indicate that non-additive gene action is affecting the phenotypes. The interplay of dominant and recessive loci only manifests in the hybrid population, either creating or concealing phenotypic variation depending on the gene action of the trait. Our study found evidence for contrasting allelic states between the two testers in several regions of the genome based on disappearance and appearance of QTL, including a dominant locus for flowering time on chromosome eight in PHJ89 compared to 3IIH6, and a putatively epistatic locus revealed for plant height in 3IIH6. Despite the strong positive correlation between the hybrid phenotypes, several loci were found in only one of the hybrid populations (Supplementary Figure 5). Perfect correlation between the test cross phenotypes would lead to the discovery of the same QTL between the two populations, yet the deviation from a one-to-one relationship between the test cross phenotypes leads to the discovery of unique QTL in the hybrid populations. Choice of tester influences hybrid performance and QTL mapping results, as evidenced by studies previously described and our findings. Despite the high correlation between the phenotypes of the hybrid populations and the expected identity

by descent between the two testers, unique QTL were discovered for each trait in each population.

Genomic prediction of hybrid phenotypes: In maize breeding programs, *per se* phenotypes are often available before hybrid varieties can be tested. Using *per se* and hybrid data from our study, we investigated the association between *per se* and hybrid flowering and height traits. We wanted to test the feasibility of predicting correlations of hybrid flowering time and height based on DH line measurements for the purposes of discarding lines that flower too late or are too tall for our breeding program. We also wanted to evaluate the predictive ability between the two hybrid populations as breeding programs often use multiple testers as materials advance through selection pipelines.

We found that the hybrids flowered earlier and were taller than their maternal DH parents, confirming heterotic relationships for flowering and height found in other studies (Flint-Garcia et al. 2009; Li et al. 2018). Previous studies have found increased predictive abilities when incorporating parental inbred information (Liang et al. 2018; Jarquin et al. 2020), and we also found moderate prediction abilities for hybrid flowering time and plant height when the models were trained using the *per se* data. As expected, the models with the highest predictive abilities were those that were trained on the data they were designed to predict, although we achieved predictive abilities between r=0.49 and r=0.55 for models predicting hybrid traits that were trained with *per se* data. Correlations between *per se* and hybrid populations do not consider the difference in magnitude between them, such as the average difference between *per se* and hybrid flowering of 90 GDU or difference in height of 71 cm. Heterosis due to small genome-wide effects produces a relatively uniform incremental decrease in flowering time and

increase in height across all lines, while variation within inbreds and within hybrids is largely due to similar large effect QTL likely in combination with undetected small effect loci. These findings are consistent with the overlapping and non-overlapping QTL that were found between the *per se* and hybrid populations because the difference between the predictive abilities for direct and *per se* to hybrid models cannot account for the dominance or epistatic effect of the tester at individual loci. In addition, the masking of *per se* QTLs within either of the hybrid populations is conceptually consistent with the lowered predictive ability of using *per se* data to predict hybrids. We also found that the errors between predicted and observed *per se* phenotypes were a source of selection error that led to discarding DH lines that would have generated acceptable hybrids.

Finally, we also used the highest associated SNP from each LOD peak as fixed effects in the genomic prediction model but found that including the fixed marker effects lowered the predictive ability compared to using only the realized relationship matrix (data not shown). This finding supports previously simulated results demonstrating that known genes are only beneficial to models when they are few in number and explain large proportions of the variance (Bernardo 2014).

Relevance to maize breeding: This method has applications in maize breeding because genomic prediction could be used to make selections prior to generating test cross seed for an entire population. Alternatively, a smaller subset of an inbred population could be grown as a model training set with several testers prior to generating larger hybrid populations. Genomic prediction could then be used to discard the poorest performing lines, which would increase genetic gain by increasing the selection intensity on the population. Overall, our results indicate that plant breeders

should be less aggressive when using predicted *per se* data to predict hybrid performance because the errors in genomic prediction can lead to discarding hybrid lines incorrectly. Plant breeders must balance their selection for maize yield with the adaptation requirements and architectural risk for root or stalk lodging when developing new inbred lines, as demonstrated by including information for flowering time and plant height in this study. Flowering time and moisture at harvest are also indications of overall relative maturity, which is an important characteristic that plant breeders use to place varieties across geographies and that farmers use to balance risk and make planting time and cultivar decisions. Our results indicate that flowering time and height have high correlations between DH lines and hybrids within these DH line-tester combinations yet experience different profiles of QTL significance across the genome. While the goal of maize breeding efforts is to increase or protect hybrid yield, most genetic research efforts focus on using inbreds to study complex traits. Understanding how traits manifest in a parental inbred versus its hybrid progeny is a critical area of maize breeding and quantitative genetics research. For example, parental *per se* measures of grain yield have been previously used to increase prediction ability of hybrid performance (Schrag et al. 2010). Deviations from the purely additive relationship of inbred flowering time or plant height to hybrid phenotype can be investigated to add to the underlying understanding of the gene action that supports genomic prediction.

CONCLUSIONS

In conclusion, several known loci were uncovered in different combinations within the *per se* and test cross sets of a MAGIC population. Dominance of one tester over the population caused the loss of a highly significant peak for anthesis, while the presence

of the other tester revealed putative epistatic variation for plant height. The six parents of the population are all members of the Stiff Stalk heterotic group, which is the canonical source of seed parent germplasm in the United States. These lines represent the diversity of both the sub-heterotic groups within the Stiff Stalk pool and the major plant breeding entities operating in the 1970's and 1980's and are no longer under intellectual property protection. In addition to dissecting the genetic architecture of these complex traits, this study provides a description of a new population resource available to maize researchers. Multi-parent populations are a unique mapping resource to study the effect of more than two parental alleles on quantitative traits, and they are a means to increase the diversity of alleles under study while managing minor allele frequency. Further, the genome assemblies of the six parents with annotation from a five-tissue transcriptome atlas (Li et al. 2021; Bornowski et al. 2021) are available for study, which increases the variety of opportunities for maize researchers. This population could be used to assay the effect of the alleles present within the population on combining ability, adaptation, genotype by environment interaction, stability, and provide a new paradigm for studying traditional and genomic selection. The practicality of leveraging linkage mapping of highly polygenic traits to make selections within breeding programs has been limited in the past, especially for traits that follow an infinitesimal model such as maize height (Peiffer et al. 2014). Nevertheless, further study of individual loci can impact plant breeding through mutational studies made possible by gene editing, in addition to current efforts in commercial plant breeding accomplished through genomic selection.

Data Availability

All supplementary tables and files have been uploaded to FigShare. Supplemental file S1 contains summary statistics regarding the exome capture, supplemental file S2 contains the exome capture probe coordinates, supplemental file S3 contains supplemental methods, supplemental file S4 is contains the unfiltered 1.8 million SNPs data, and supplemental file S5 contains the control folder for mapping in R/qtl2, including marker maps, genotypes, phenotypes, and cross information. Supplemental table ST1 contains descriptions of the lines in the study, ST2 contains details about the field experiments, ST3 contains plot-based data, ST4 contains information about the stage one models used for calculating BLUE phenotypes, ST5 contains the BLUE phenotypes, ST6 contains the reference range haplotype IDs, and ST7 contains all significant QTL peaks. Raw exome capture and GBS sequence reads are available in the National Center for Biotechnology Information Short Read Archive under BioProjects PRJNA781987 and PRJNA781986 respectively.

Acknowledgements

The authors acknowledge Mona Mazaheri and Alden Perkins for support with tissue sampling, Brieanne Vaillancourt and Joshua C. Wood for assistance with exome capture sequence data processing, Zachary Miller, Lynn Johnson, Joseph Gage for advice in building the WI-SS-MAGIC Practical Haplotype Graph, Dylan Schoemaker for helpful discussion on genomic prediction and the manuscript, and AgReliant Genetics for providing doubled haploid induction as in-kind support. The authors utilized the University of Wisconsin – Madison Biotechnology Center's DNA Sequencing Facility (Research Resource Identifier – RRID:SCR_017759) to extract DNA, generate GBS

libraries, and sequence GBS libraries. The UWBC is a Licensed Service Provider for internal and external clients, providing GBS services under license from Keygene N.V. which owns patents and patent applications protecting its Sequence Based Genotyping technologies.

Funding

This work was supported and funded by the U.S. Department of Energy Great Lakes Bioenergy Research Center (DOE BER Office of Science DE-FC02-07ER64494) to CRB, SMK, NdL; USDOE ARPA-E ROOTS Award Number DE-AR0000821, National Corn Growers Association and Iowa Corn Growers Association support to DCL, NdL, SMK; the D.C. Smith Wisconsin Distinguished Graduate Fellowship to KJM; the National Institute of Food and Agriculture, United States Department of Agriculture Hatch 1013139 and 1022702 project to SMK, and National Institutes of Health grant R01GM070683 to KWB. The work (proposal: 10.46936/10.25585/60000838) conducted by the U.S. Department of Energy Joint Genome Institute (https://ror.org/04xm1d337), a DOE Office of Science User Facility, is supported by the Office of Science of the U.S. Department of Energy operated under Contract No. DE-AC02-05CH11231.

Conflict of interest

The authors declare no conflicts of interest.

REFERENCES

Alter P, Bircheneder S, Zhou L-Z, Schlüter U, Gahrtz M, Sonnewald U, Dresselhaus T. 2016. Flowering time-regulated genes in maize include the transcription factor *ZmMADS1*. Plant Physiol. 172(1):389–404. https://doi.org/10.1104/pp.16.00285

855 Austin DF, Lee M, Veldboom LR. 2001. Genetic mapping in maize with hybrid progeny
856 across testers and generations: plant height and flowering. Theor Appl Genet.
857 102(1):163–176. https://doi.org/10.1007/s001220051632

858 Bauer E, Falque M, Walter H, Bauland C, Camisan C, Campo L, Meyer N, Ranc N,
859 Rincent R, Schipprack W, et al. 2013. Intraspecific variation of recombination rate
860 in maize. Genome Biology. 14(9):R103. https://doi.org/10.1186/gb-2013-14-9-
861 r103

862 Baum ME, Archontoulis SV, Licht MA. 2019. Planting date, hybrid maturity, and weather
863 effects on maize yield and crop stage. Agron J. 111(1):303–313.
864 https://doi.org/10.2134/agronj2018.04.0297

865 Bernardo R. 2014. Genomewide selection when major genes are known. Crop Sci.
866 54(1):68–75. https://doi.org/10.2135/cropsci2013.05.0315

867 Bornowski N, Michel KJ, Hamilton JP, Ou S, Seetharam AS, Jenkins J, Grimwood J,
868 Plott C, Shu S, Talag J, et al. 2021. Genomic variation within the maize stiff-stalk
869 heterotic germplasm pool. Plant Genome. 14(3):e20114.
870 https://doi.org/10.1002/tpg2.20114

871 Bradbury PJ, Casstevens T, Jensen SE, Johnson LC, Miller ZR, Monier B, Romay MC,
872 Song B, Buckler ES. 2021. The Practical Haplotype Graph, a platform for storing
873 and using pangenomes for imputation. bioRxiv [Internet]. [accessed 2021 Oct
874 25]. https://doi.org/10.1101/2021.08.27.457652

875 Bradbury PJ, Zhang Z, Kroon DE, Casstevens TM, Ramdoss Y, Buckler ES. 2007.
876 TASSEL: Software for association mapping of complex traits in diverse samples.
877 Bioinformatics. 23(19):2633–2635. https://doi.org/10.1093/bioinformatics/btm308

878 Brohammer AB, Kono TJY, Springer NM, McGaugh SE, Hirsch CN. 2018. The limited
879 role of differential fractionation in genome content variation and function in maize
880 (*Zea mays* L.) inbred lines. Plant J. 93(1):131–141.
881 https://doi.org/10.1111/tpj.13765

882 Broman KW, Gatti DM, Simecek P, Furlotte NA, Prins P, Sen Ś, Yandell BS, Churchill
883 GA. 2019. R/qtl2: Software for mapping quantitative trait loci with high-
884 dimensional data and multiparent populations. Genetics. 211(2):495–502.
885 https://doi.org/10.1534/genetics.118.301595

886 Broman KW, Sen Ś. 2009. *A Guide to QTL Mapping with R/qtl*. New York: Springer.

887 Buckler ES, Holland JB, Bradbury PJ, Acharya CB, Brown PJ, Browne C, Ersoz E, Flint-
888 Garcia S, Garcia A, Glaubitz JC, et al. 2009. The genetic architecture of maize
889 flowering time. Science. 325(5941):714–718.
890 https://doi.org/10.1126/science.1174276

891 Butler DG, Cullis BR, Gilmour AR, Gogel BG, Thompson R. 2017. Asreml-R reference
892 manual version 4. Hemel Hempstead, HP1 1ES, UK: VSN International Ltd.

893 Cai H, Chu Q, Gu R, Yuan L, Liu J, Zhang X, Chen F, Mi G, Zhang F. 2012.
894 Identification of QTLs for plant height, ear height and grain yield in maize (*Zea*

mays L.) in response to nitrogen and phosphorus supply. Plant Breed. 131(4):502–510. https://doi.org/10.1111/j.1439-0523.2012.01963.x

Chen Y, Hou M, Liu L, Wu S, Shen Y, Ishiyama K, Kobayashi M, McCarty DR, Tan B-C. 2014. The maize *DWARF1* encodes a gibberellin 3-oxidase and is dual localized to the nucleus and cytosol. Plant Physiol. 166(4):2028–2039. https://doi.org/10.1104/pp.114.247486

Cheng R, Palmer AA. 2013. A simulation study of permutation, bootstrap, and gene dropping for assessing statistical significance in the case of unequal relatedness. Genetics. 193(3):1015–1018. https://doi.org/10.1534/genetics.112.146332

Churchill GA, Doerge RW. 1994. Empirical threshold values for quantitative trait mapping. Genetics. 138(3):963–971. https://doi.org/10.1093/genetics/138.3.963

Colasanti J, Yuan Z, Sundaresan V. 1998. The *indeterminate* gene encodes a zinc finger protein and regulates a leaf-generated signal required for the transition to flowering in maize. Cell. 93(4):593–603. https://doi.org/10.1016/S0092-8674(00)81188-5

Cullis BR, Smith AB, Coombes NE. 2006. On the design of early generation variety trials with correlated data. J Agric Biol Environ Stat. 11(4):381–393. https://doi.org/10.1198/108571106X154443

Dekalb Plant Genetics. 1994. Corn “3IIH6” [Internet]. [accessed 2021 Jul 15]. https://apps.ams.usda.gov/CMS/AdobeImages/009300087.pdf

915 Dell'Acqua M, Gatti DM, Pea G, Cattonaro F, Coppens F, Magris G, Hlaing AL, Aung
916 HH, Nelissen H, Baute J, et al. 2015. Genetic properties of the MAGIC maize
917 population: a new platform for high definition QTL mapping in *Zea mays*.
918 Genome Biol. 16(1):167. https://doi.org/10.1186/s13059-015-0716-z

919 Ding J, Zhang L, Chen J, Li X, Li Y, Cheng H, Huang R, Zhou B, Li Z, Wang J, Wu J.
920 2015. Genomic dissection of leaf angle in maize (*Zea mays* L.) using a four-way
921 cross mapping population. PLOS ONE. 10(10):e0141619.
922 https://doi.org/10.1371/journal.pone.0141619

923 Ding X, Wu X, Chen L, Li C, Shi Y, Song Y, Zhang D, Wang T, Li Yu, Liu Z, Li Yong-
924 xiang. 2016. Both major and minor QTL associated with plant height can be
925 identified using near-isogenic lines in maize. Euphytica. 213(1):21.
926 https://doi.org/10.1007/s10681-016-1825-9

927 Duvick DN, Cassman KG. 1999. Post–green revolution trends in yield potential of
928 temperate maize in the north-central United States. Crop Sci. 39(6):1622–1630.
929 https://doi.org/10.2135/cropsci1999.3961622x

930 Elshire RJ, Glaubitz JC, Sun Q, Poland JA, Kawamoto K, Buckler ES, Mitchell SE.
931 2011. A robust, simple genotyping-by-sequencing (GBS) approach for high
932 diversity species. PLOS ONE. 6(5):e19379.
933 https://doi.org/10.1371/journal.pone.0019379

934 Endelman JB. 2011. Ridge regression and other kernels for genomic selection with R
935 package rrblup. Plant Genome. 4(3):250–255.
936 https://doi.org/10.3835/plantgenome2011.08.0024

937 Ewels P, Magnusson M, Lundin S, Käller M. 2016. MultiQC: summarize analysis results
938 for multiple tools and samples in a single report. Bioinformatics. 32(19):3047–
939 3048. https://doi.org/10.1093/bioinformatics/btw354

940 Falconer DS, Mackay TFC. 1989. *Introduction to Quantitative Genetics*. 3th ed. New
941 York, NY: John Wiley and Sons, Inc.

942 Flint-Garcia SA, Buckler ES, Tiffin P, Ersoz E, Springer NM. 2009. Heterosis is
943 prevalent for multiple traits in diverse maize germplasm. PLoS ONE.
944 4(10):e7433. https://doi.org/10.1371/journal.pone.0007433

945 Frascaroli E, Canè MA, Pè ME, Pea G, Morgante M, Landi P. 2009. QTL detection in
946 maize testcross progenies as affected by related and unrelated testers. Theor
947 Appl Genet. 118(5):993–1004. https://doi.org/10.1007/s00122-008-0956-3

948 Gardner KA, Wittern LM, Mackay IJ. 2016. A highly recombined, high-density, eight-
949 founder wheat MAGIC map reveals extensive segregation distortion and genomic
950 locations of introgression segments. Plant Biotechnol J. 14(6):1406–1417.
951 https://doi.org/10.1111/pbi.12504

952 Giraud H, Bauland C, Falque M, Madur D, Combes V, Jamin P, Monteil C, Laborde J,
953 Palaffre C, Gaillard A, et al. 2017. Reciprocal Genetics: Identifying QTL for
954 General and Specific Combining Abilities in Hybrids Between Multiparental

955 Populations from Two Maize (*Zea mays* L.) Heterotic Groups. Genetics.
956 207(3):1167–1180. https://doi.org/10.1534/genetics.117.300305

957 Guo L, Wang X, Zhao M, Huang C, Li C, Li D, Yang CJ, York AM, Xue W, Xu G, et al.
958 2018. Stepwise cis-regulatory changes in *ZCN8* contribute to maize flowering-
959 time adaptation. Curr Biol. 28(18):3005-3015.e4.
960 https://doi.org/10.1016/j.cub.2018.07.029

961 Hayes BJ, Visscher PM, Goddard ME. 2009. Increased accuracy of artificial selection
962 by using the realized relationship matrix. Genet Res. 91(1):47–60.
963 https://doi.org/10.1017/S0016672308009981

964 Hinze LL, Lamkey KR. 2003. Absence of epistasis for grain yield in elite maize hybrids.
965 Crop Sci. 43(1):46–56. https://doi.org/10.2135/cropsci2003.4600

966 Huang C, Sun H, Xu D, Chen Q, Liang Y, Wang X, Xu G, Tian J, Wang C, Li D, et al.
967 2018. *ZmCCT9* enhances maize adaptation to higher latitudes. Proc Natl Acad
968 Sci. 115(2):E334–E341. https://doi.org/10.1073/pnas.1718058115

969 Hung H-Y, Shannon LM, Tian F, Bradbury PJ, Chen C, Flint-Garcia SA, McMullen MD,
970 Ware D, Buckler ES, Doebley JF, Holland JB. 2012. *ZmCCT* and the genetic
971 basis of day-length adaptation underlying the postdomestication spread of maize.
972 Proc Natl Acad Sci. 109(28):E1913–E1921.
973 https://doi.org/10.1073/pnas.1203189109

974 Huynh B-L, Ehlers JD, Huang BE, Muñoz-Amatriaín M, Lonardi S, Santos JRP, Ndeve
975 A, Batieno BJ, Boukar O, Cisse N, et al. 2018. A multi-parent advanced

976 generation inter-cross (MAGIC) population for genetic analysis and improvement
977 of cowpea (*Vigna unguiculata* L. Walp.). Plant J. 93(6):1129–1142.
978 https://doi.org/10.1111/tpj.13827

979 Jarquin D, Howard R, Liang Z, Gupta SK, Schnable JC, Crossa J. 2020. Enhancing
980 hybrid prediction in pearl millet using genomic and/or multi-environment
981 phenotypic information of inbreds. Front Genet. 10:1294.
982 https://doi.org/10.3389/fgene.2019.01294

983 Jiménez-Galindo JC, Malvar RA, Butrón A, Santiago R, Samayoa LF, Caicedo M,
984 Ordás B. 2019. Mapping of resistance to corn borers in a MAGIC population of
985 maize. BMC Plant Biol. 19(1):431. https://doi.org/10.1186/s12870-019-2052-z

986 Jin M, Liu X, Jia W, Liu H, Li W, Peng Y, Du Y, Wang Y, Yin Y, Zhang X, et al. 2018.
987 *ZmCOL3*, a *CCT* gene represses flowering in maize by interfering with the
988 circadian clock and activating expression of *ZmCCT*. J Integr Plant Biol.
989 60(6):465–480. https://doi.org/10.1111/jipb.12632

990 Khush GS. 2001. Green revolution: the way forward. Nat Rev Genet. 2(10):815–822.
991 https://doi.org/10.1038/35093585

992 Kover PX, Valdar W, Trakalo J, Scarcelli N, Ehrenreich IM, Purugganan MD, Durrant C,
993 Mott R. 2009. A multiparent advanced generation inter-cross to fine-map
994 quantitative traits in *Arabidopsis thaliana*. Mauricio R, editor. PLoS Genet.
995 5(7):e1000551. https://doi.org/10.1371/journal.pgen.1000551

Li C, Li Yongxiang, Bradbury PJ, Wu X, Shi Y, Song Y, Zhang D, Rodgers-Melnick E, Buckler ES, Zhang Z, et al. 2015. Construction of high-quality recombination maps with low-coverage genomic sequencing for joint linkage analysis in maize. BMC Biol. 13(1):78. https://doi.org/10.1186/s12915-015-0187-4

Li C, Li Yongxiang, Sun B, Peng B, Liu C, Liu Z, Yang Z, Li Q, Tan W, Zhang Y, et al. 2013. Quantitative trait loci mapping for yield components and kernel-related traits in multiple connected RIL populations in maize. Euphytica. 193(3):303–316. https://doi.org/10.1007/s10681-013-0901-7

Li L, Xu X, Jin W, Chen S. 2009. Morphological and molecular evidences for DNA introgression in haploid induction via a high oil inducer CAUHOI in maize. Planta. 230(2):367–376. https://doi.org/10.1007/s00425-009-0943-1

Li Z, Coffey L, Garfin J, Miller ND, White MR, Spalding EP, Leon N de, Kaeppler SM, Schnable PS, Springer NM, Hirsch CN. 2018. Genotype-by-environment interactions affecting heterosis in maize. PLOS ONE. 13(1):e0191321. https://doi.org/10.1371/journal.pone.0191321

Li Z, Zhou P, Coletta RD, Zhang T, Brohammer AB, O'Connor CH, Vaillancourt B, Lipzen A, Daum C, Barry K, et al. 2021. Single-parent expression drives dynamic gene expression complementation in maize hybrids. Plant J. 105(1):93–107. https://doi.org/10.1111/tpj.15042

Liang Y, Liu Q, Wang X, Huang C, Xu G, Hey S, Lin H-Y, Li C, Xu D, Wu L, et al. 2019. *ZmMADS69* functions as a flowering activator through the *ZmRap2.7-ZCN8*

regulatory module and contributes to maize flowering time adaptation. New Phytol. 221(4):2335–2347. https://doi.org/10.1111/nph.15512

Liang Z, Gupta SK, Yeh C-T, Zhang Y, Ngu DW, Kumar R, Patil HT, Mungra KD, Yadav DV, Rathore A, et al. 2018. Phenotypic data from inbred parents can improve genomic prediction in pearl millet hybrids. G3 Genes|Genomes|Genetics. 8(7):2513–2522. https://doi.org/10.1534/g3.118.200242

Lübberstedt T, Melchinger AE, Schön CC, Utz HF, Klein D. 1997. QTL mapping in testcrosses of European flint lines of maize: i. Comparison of different testers for forage yield traits. Crop Sci. 37(3):921–931. https://doi.org/10.2135/cropsci1997.0011183X003700030037x

Mahan AL, Murray SC, Klein PE. 2018. Four-parent maize (FPM) population: development and phenotypic characterization. Crop Sci. 58(3):1106–1117. https://doi.org/10.2135/cropsci2017.07.0450

Makarevitch I, Thompson A, Muehlbauer GJ, Springer NM. 2012. *Brd1* gene in maize encodes a brassinosteroid c-6 oxidase. PLoS ONE. 7(1):e30798. https://doi.org/10.1371/journal.pone.0030798

Marçais G, Delcher AL, Phillippy AM, Coston R, Salzberg SL, Zimin A. 2018. MUMmer4: a fast and versatile genome alignment system. PLOS Comput Biol. 14(1):e1005944. https://doi.org/10.1371/journal.pcbi.1005944

1036 Martin M. 2011. Cutadapt removes adapter sequences from high-throughput
1037 sequencing reads. EMBnet.journal. 17(1):10–12.
1038 https://doi.org/10.14806/ej.17.1.200

1039 Mascher M, Richmond TA, Gerhardt DJ, Himmelbach A, Clissold L, Sampath D, Ayling
1040 S, Steuernagel B, Pfeifer M, D'Ascenzo M, et al. 2013. Barley whole exome
1041 capture: a tool for genomic research in the genus *Hordeum* and beyond. Plant J.
1042 76(3):494–505. https://doi.org/10.1111/tpj.12294

1043 Mazaheri M, Heckwolf M, Vaillancourt B, Gage JL, Burdo B, Heckwolf S, Barry K,
1044 Lipzen A, Ribeiro CB, Kono TJY, et al. 2019. Genome-wide association analysis
1045 of stalk biomass and anatomical traits in maize. BMC Plant Biol. 19(1):1–17.
1046 https://doi.org/10.1186/s12870-019-1653-x

1047 Melchinger AE, Utz HF, Schön CC. 1998. Quantitative trait locus (QTL) mapping using
1048 different testers and independent population samples in maize reveals low power
1049 of QTL detection and large bias in estimates of QTL effects. Genetics.
1050 149(1):383–403.

1051 Mihaljevic R, Utz HF, Melchinger AE. 2005. No evidence for epistasis in hybrid and per
1052 se performance of elite European flint maize inbreds from generation means and
1053 QTL analyses. Crop Sci. 45(6):2605–2613.
1054 https://doi.org/10.2135/cropsci2004.0760

1055 Mikel MA. 2011. Genetic composition of contemporary U.S. commercial dent corn
1056 germplasm. Crop Sci. 51(2):592–599.
1057 https://doi.org/10.2135/cropsci2010.06.0332

1058 Muszynski MG, Dam T, Li B, Shirbroun DM, Hou Z, Bruggemann E, Archibald R,
1059 Ananiev EV, Danilevskaya ON. 2006. *delayed flowering1* encodes a basic
1060 leucine zipper protein that mediates floral inductive signals at the shoot apex in
1061 maize. Plant Physiol. 142(4):1523–1536. https://doi.org/10.1104/pp.106.088815

1062 Ogawa D, Nonoue Y, Tsunematsu H, Kanno N, Yamamoto T, Yonemaru J-I. 2018.
1063 Discovery of QTL alleles for grain shape in the Japan-MAGIC rice population
1064 using haplotype information. G3 Genes|Genomes|Genetics. 8(11):3559–3565.
1065 https://doi.org/10.1534/g3.118.200558

1066 Ongom PO, Ejeta G. 2018. Mating design and genetic structure of a multi-parent
1067 advanced generation intercross (MAGIC) population of sorghum (*Sorghum*
1068 *bicolor* (L.) Moench). G3 Genes|Genomes|Genetics. 8(1):331–341.
1069 https://doi.org/10.1534/g3.117.300248

1070 Pascual L, Desplat N, Huang BE, Desgroux A, Bruguier L, Bouchet J-P, Le QH,
1071 Chauchard B, Verschave P, Causse M. 2015. Potential of a tomato MAGIC
1072 population to decipher the genetic control of quantitative traits and detect causal
1073 variants in the resequencing era. Plant Biotechnol J. 13(4):565–577.
1074 https://doi.org/10.1111/pbi.12282

1075 Peiffer JA, Romay MC, Gore MA, Flint-Garcia SA, Zhang Z, Millard MJ, Gardner CAC,
1076 McMullen MD, Holland JB, Bradbury PJ, Buckler ES. 2014. The genetic
1077 architecture of maize height. Genetics. 196(4):1337–1356.
1078 https://doi.org/10.1534/genetics.113.159152

1079 Pioneer Hi-Bred International Inc. 1992. Corn “PHJ89” [Internet]. [accessed 2021 Jul
1080 15]. https://apps.ams.usda.gov/CMS/AdobeImages/009100092.pdf

1081 Poland JA, Brown PJ, Sorrells ME, Jannink J-L. 2012. Development of high-density
1082 genetic maps for barley and wheat using a novel two-enzyme genotyping-by-
1083 sequencing approach. PLoS ONE. 7(2):e32253.
1084 https://doi.org/10.1371/journal.pone.0032253

1085 Pope R. 2008. Calculating degree days. Iowa State Univ Ext Outreach Integr Crop
1086 Manag [Internet]. [accessed 2021 Apr 22].
1087 https://crops.extension.iastate.edu/cropnews/2008/04/calculating-degree-days

1088 RCoreTeam. 2018. R: A language and environment for statistical computing. [place
1089 unknown].

1090 Rogers AR, Dunne JC, Romay C, Bohn M, Buckler ES, Ciampitti IA, Edwards J, Ertl D,
1091 Flint-Garcia S, Gore MA, et al. 2021. The importance of dominance and
1092 genotype-by-environment interactions on grain yield variation in a large-scale
1093 public cooperative maize experiment. G3 Genes|Genomes|Genetics. 11(2).
1094 https://doi.org/10.1093/g3journal/jkaa050

1095 Russell WA. 1972. PL-17, Maize. Crop Sci Regist. 12(5):721.

1096 Russell WA. 1979. Registration of B84 parental line of maize. PL-50, Maize. Crop Sci
1097 Regist. 19(4):566.

1098 Saghai-Maroof MA, Soliman KM, Jorgensen RA, Allard RW. 1984. Ribosomal DNA
1099 spacer-length polymorphisms in barley: Mendelian inheritance, chromosomal
1100 location, and population dynamics. Proc Natl Acad Sci. 81(24):8014–8018.
1101 https://doi.org/10.1073/pnas.81.24.8014

1102 Salas Fernandez MG, Becraft PW, Yin Y, Lübberstedt T. 2009. From dwarves to
1103 giants? Plant height manipulation for biomass yield. Trends Plant Sci. 14(8):454–
1104 461. https://doi.org/10.1016/j.tplants.2009.06.005

1105 Salvi S, Sponza G, Morgante M, Tomes D, Niu X, Fengler KA, Meeley R, Ananiev EV,
1106 Svitashev S, Bruggemann E, et al. 2007. Conserved noncoding genomic
1107 sequences associated with a flowering-time quantitative trait locus in maize. Proc
1108 Natl Acad Sci U S A. 104(27):11376–11381.
1109 https://doi.org/10.1073/pnas.0704145104

1110 Sannemann W, Huang BE, Mathew B, Léon J. 2015. Multi-parent advanced generation
1111 inter-cross in barley: high-resolution quantitative trait locus mapping for flowering
1112 time as a proof of concept. Mol Breed. 35(3):86. https://doi.org/10.1007/s11032-
1113 015-0284-7

1114 Schrag TA, Möhring J, Melchinger AE, Kusterer B, Dhillon BS, Piepho H-P, Frisch M.
1115 2010. Prediction of hybrid performance in maize using molecular markers and

joint analyses of hybrids and parental inbreds. Theor Appl Genet. 120(2):451–461. https://doi.org/10.1007/s00122-009-1208-x

Schwarz G. 1978. Estimating the dimension of a model. Ann Stat. 6(2):461–464.

Scott MF, Ladejobi O, Amer S, Bentley AR, Biernaskie J, Boden SA, Clark M, Dell'Acqua M, Dixon LE, Filippi CV, et al. 2020. Multi-parent populations in crops: a toolbox integrating genomics and genetic mapping with breeding. Heredity. 125(6):396–416. https://doi.org/10.1038/s41437-020-0336-6

Seye AI, Bauland C, Giraud H, Mechin V, Reymond M, Charcosset A, Moreau L. 2019. Quantitative trait loci mapping in hybrids between Dent and Flint maize multiparental populations reveals group-specific QTL for silage quality traits with variable pleiotropic effects on yield. Theor Appl Genet. 132(5):1523–1542. https://doi.org/10.1007/s00122-019-03296-2

Stephenson E, Estrada S, Meng X, Ourada J, Muszynski MG, Habben JE, Danilevskaya ON. 2019. Over-expression of the photoperiod response regulator *ZmCCT10* modifies plant architecture, flowering time and inflorescence morphology in maize. PLOS ONE. 14(2):e0203728. https://doi.org/10.1371/journal.pone.0203728

Tibbs Cortes L, Zhang Z, Yu J. 2021. Status and prospects of genome-wide association studies in plants. Plant Genome. 14(1):e20077. https://doi.org/10.1002/tpg2.20077

Troyer AF. 1999. (1999) Background of U.S. Hybrid Corn. Crop Sci. 39:601–626.

1137 Troyer AF. 2004. Background of U.S. Hybrid Corn II: Breeding, Climate, and Food. Crop
1138 Sci. 44(2):370–380. https://doi.org/10.2135/cropsci2004.3700

1139 Wallace JG, Zhang X, Beyene Y, Semagn K, Olsen M, Prasanna BM, Buckler ES.
1140 2016. Genome-wide association for plant height and flowering time across 15
1141 tropical maize populations under managed drought stress and well-watered
1142 conditions in sub-Saharan Africa. Crop Sci. 56(5):2365–2378.
1143 https://doi.org/10.2135/cropsci2015.10.0632

1144 Wang L, Zhou Z, Li R, Weng J, Zhang Q, Li Xinghua, Wang B, Zhang W, Song W, Li
1145 Xinhai. 2021. Mapping QTL for flowering time-related traits under three plant
1146 densities in maize. Crop J. 9(2):372–379. https://doi.org/10.1016/j.cj.2020.07.009

1147 Wang X, Wu Liuji, Zhang S, Wu Liancheng, Ku L, Wei X, Xie L, Chen Y. 2011. Robust
1148 expression and association of *ZmCCA1* with circadian rhythms in maize. Plant
1149 Cell Rep. 30(7):1261–1272. https://doi.org/10.1007/s00299-011-1036-8

1150 White MR, Mikel MA, de Leon N, Kaeppler SM. 2020. Diversity and heterotic patterns in
1151 North American proprietary dent maize germplasm. Crop Sci. 60(1):100–114.
1152 https://doi.org/10.1002/csc2.20050

1153 Xiao Y, Jiang S, Cheng Q, Wang Xiaqing, Yan Jun, Zhang R, Qiao F, Ma C, Luo J, Li
1154 W, et al. 2021. The genetic mechanism of heterosis utilization in maize
1155 improvement. Genome Biol. 22(1):148. https://doi.org/10.1186/s13059-021-
1156 02370-7

1157 Xu J, Liu Y, Liu J, Cao M, Wang J, Lan H, Xu Y, Lu Y, Pan G, Rong T. 2012. The
1158 genetic architecture of flowering time and photoperiod sensitivity in maize as
1159 revealed by QTL review and meta analysis. J Integr Plant Biol. 54(6):358–373.
1160 https://doi.org/10.1111/j.1744-7909.2012.01128.x

1161 Yang J, Zaitlen NA, Goddard ME, Visscher PM, Price AL. 2014. Advantages and pitfalls
1162 in the application of mixed-model association methods. Nat Genet. 46(2):100–
1163 106. https://doi.org/10.1038/ng.2876

1164 Yu J, Holland JB, McMullen MD, Buckler ES. 2008. Genetic design and statistical power
1165 of nested association mapping in maize. Genetics. 178(1):539–551.
1166 https://doi.org/10.1534/genetics.107.074245

1167

1168 **Figure Captions**

1169 Figure 1: Distributions of phenotypic BLUEs and heritabilities

1170 Distributions for anthesis growing degree units (GDU) and plant height for the UW-
1171 MAGIC-SS *per se* population, SS-3IIH6 hybrid population, and SS-PHJ89 hybrid
1172 population. Trait heritabilities are in the upper left of each plot. Population parent BLUEs
1173 are plotted as colored lines behind each distribution.

1174 Figure 2: Phenotypic correlations between populations

1175 Scatterplots of BLUEs demonstrate the positive correlation within traits, between
1176 populations. Pearson correlations are shown in the lower right.

Figure 3: Population genetic characteristics

(A) Distribution of the number of consensus haplotypes found per reference range. (B) Multidimensional scale plot using 1.8 million genic SNPs, with the population parents plotted in red. (C) Distribution of the minor allele frequencies for 100,000 filtered numeric SNPs, with vertical lines plotted at expected peaks of 1/6 and 2/6. (D) Histogram of the number of crossovers per individual for the two population subsets prior to filtering lines with high total crossovers. Six lines with more than 600 crossovers are not included. Vertical lines indicate the thresholds used for discarding lines at 150 crossovers for subset A (generated using three meioses) and 250 crossovers for subset B (generated using five meioses).

Figure 4: Anthesis GDU QTL mapping

Population specific LOD scores are plotted for each panel. Dashed vertical lines show known flowering time genes. (A) QTL peaks for the *per se* population for each of the ten chromosomes. (B) QTL peaks for chromosome eight of the SS-3IIH6 population and the DH lines that were used to generate the population. (C) QTL peaks for chromosome eight of the SS-PHJ89 population and the DH lines that were used to generate the population.

Figure 5: Founder anthesis GDU QTL BLUP effects

BLUP effects for each parental contribution are plotted for the two chromosomes containing the most significant peaks for flowering time. Vertical lines are plotted denoting three major flowering time loci.

Figure 6: Plant height QTL mapping

Population specific LOD scores are plotted for each panel. Dashed vertical lines show known height genes. (A) QTL peaks for the *per se* population for each of the ten chromosomes. (B) QTL peaks for three chromosomes of the SS-3IIH6 population and the DH lines that were used to generate the population. (C) QTL peaks for three chromosomes of the SS-PHJ89 population and the DH lines that were used to generate the population.

Figure 7: Predictive abilities for direct and indirect genomic prediction models

Legend: Predictive abilities for 100 replications of each model. Direct models were trained using the population phenotype they would predict, while indirect models were trained with the *per se* or opposite hybrid population and used to predict each phenotype.

Supplemental Figure 1: Phenotypic correlations between traits

Scatterplots of BLUEs demonstrate the positive correlation between traits, within populations. Pearson correlations are shown in the upper left.

Supplemental Figure 2: Haplotypes for six representative UW-SS-MAGIC lines

Lines in the top row are from Subset A, and each have 60 crossovers. Lines in the bottom row are from Subset B, and each have 103 crossovers. Genomic areas plotted in white did not have a founder probability rise above 50% in that region.

Supplemental Figure 3: QTL linkage mapping and GWAS for flowering time

(A) Anthesis GDU QTL peaks and SNP association results in the *per se* population. (B) Silking GDU QTL peaks and SNP association results in the *per se* population.

Supplemental Figure 4: QTL linkage mapping and GWAS for plant and ear height

(A) Plant height QTL peaks and SNP association results in the *per se* population. (B) Ear height QTL peaks and SNP association results in the *per se* population.

Supplemental Figure 5: All significant QTL identified for flowering time and plant height

Significant loci are plotted for flowering and height traits for the *per se* population, SS-3IIH6 hybrid population, and SS-PHJ89 hybrid populations. Previously characterized flowering and height loci are plotted as dashed vertical lines. To declare two significant loci under one large QTL peak, the LOD score was required to drop by at least five.

Supplemental Figure 6: Founder plant height BLUP effects

QTL BLUP effects with +/- 2 standard errors at the most significant locus for SS-3IIH6 plant height in the *per se*, SS-3IIH6, and SS-PHJ89 populations on chromosomes six. This QTL was not significant in the *per se* or SS-PHJ89 populations.

Supplemental Figure 7: Observed vs predicted phenotypes and discard accuracy

(A) Scatterplot of observed vs predicted anthesis GDU for the *per se* population. To select for adaptation to Wisconsin, our breeding program discards the latest lines of a population. Lines in the top 15% of both observed and predicted anthesis values (i.e. flower the latest) are colored in green, lines that flower in the latest 15% of predicted values are plotted in pink, and lines that flower in the latest 15% of observed values are plotted in blue. Color is recorded for each DH line name. (B) Using the DH line color scheme from A, the hybrid phenotypes are plotted for SS-3IIH6 and SS-PHJ89. (C) Scatterplot of observed vs predicted plant height for the *per se* population. Our breeding

program discards the tallest members of the population. Lines are colored in the same manner as Panel A. (D) Using the DH line color scheme from C, the hybrid phenotypes are plotted for SS-3IIH6 and SS-PHJ89.

Supplemental Figure 8: Box plots for each *per se* digenic class for two flowering time loci

The study of epistasis is difficult due to low sample sizes of each digenic class. Each panel represents a digenic class for the two most significant *per se* anthesis GDU loci on chromosomes three and eight. The population wide mean is plotted as a red dot on each panel. Sample size for each class is in the lower left corner.

Supplemental Figure 9: Bar plots for each SS-3IIH6 digenic class for two plant height loci

The study of epistasis is difficult due to low sample sizes of each digenic class. Each panel represents a digenic class for two significant SS-3IIH6 plant height loci on chromosomes one and six. The population wide mean is plotted as a red dot on each panel. Sample size for each class is in the lower left corner. Some digenic classes have no observed individuals.

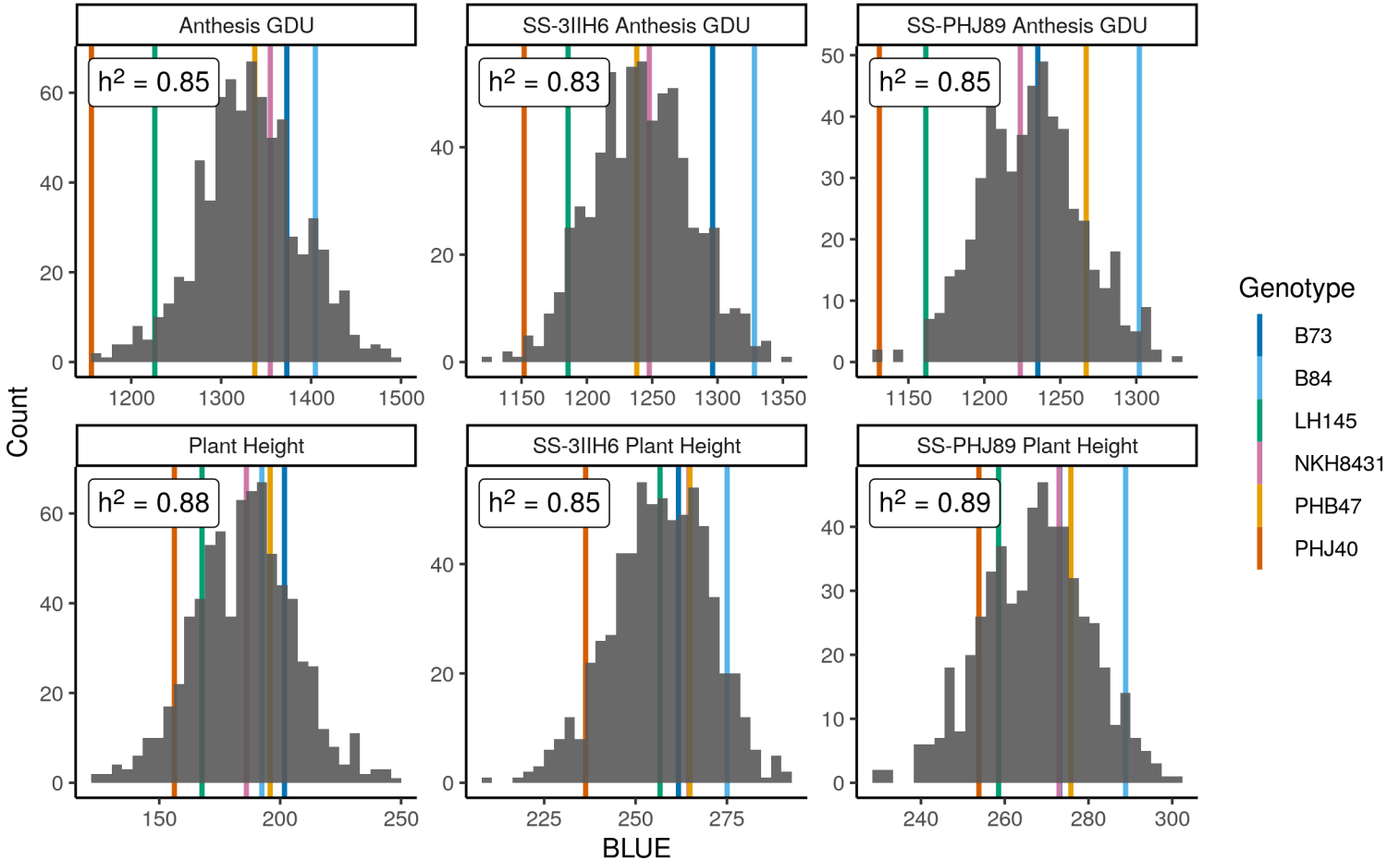
Anthesis GDU
h2 = 0.85
SS-3IIH6 Anthesis GDU
h2 = 0.83
SS-PHJ89 Anthesis GDU
h2 = 0.85
Plant Height
h2 = 0.88
SS-3IIH6 Plant Height
h2 = 0.85
SS-PHJ89 Plant Height
h2 = 0.89
Count
BLUE
Genotype
B73
B84
LH145
NKH8431
PHB47
PHJ40

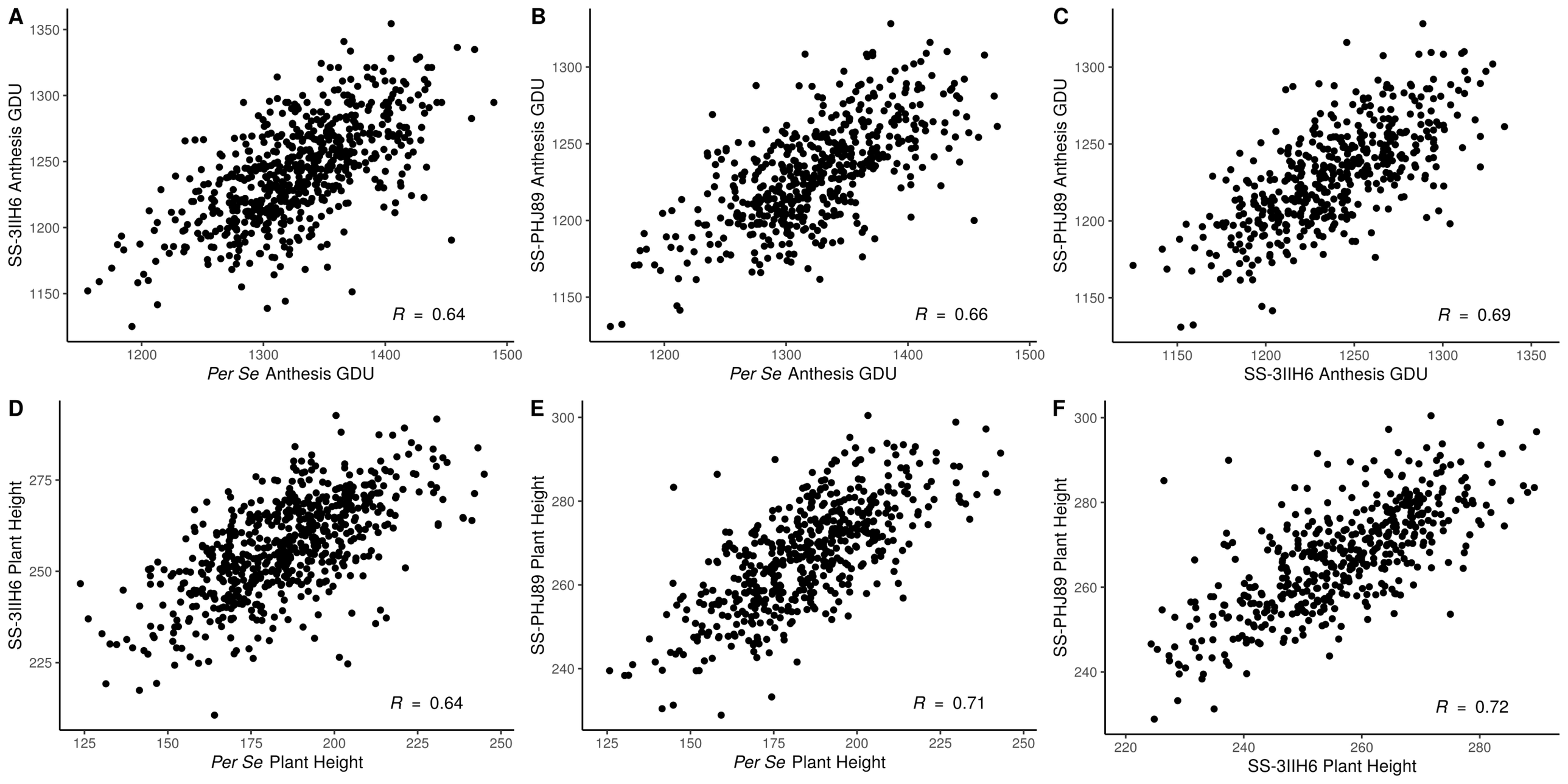
A
SS-3IIH6 Anthesis GDU
1350
1300
1250
1200
1150
R = 0.64
1200
1300
1400
1500
Per Se Anthesis GDU
B
SS-PHJ89 Anthesis GDU
1300
1250
1200
1150
R = 0.66
1200
1300
1400
1500
Per Se Anthesis GDU
C
SS-PHJ89 Anthesis GDU
1300
1250
1200
1150
R = 0.69
1150
1200
1250
1300
1350
SS-3IIH6 Anthesis GDU
D
SS-3IIH6 Plant Height
275
250
225
R = 0.64
125
150
175
200
225
250
Per Se Plant Height
E
SS-PHJ89 Plant Height
300
280
260
240
R = 0.71
125
150
175
200
225
250
Per Se Plant Height
F
SS-PHJ89 Plant Height
300
280
260
240
R = 0.72
220
240
260
280
SS-3IIH6 Plant Height

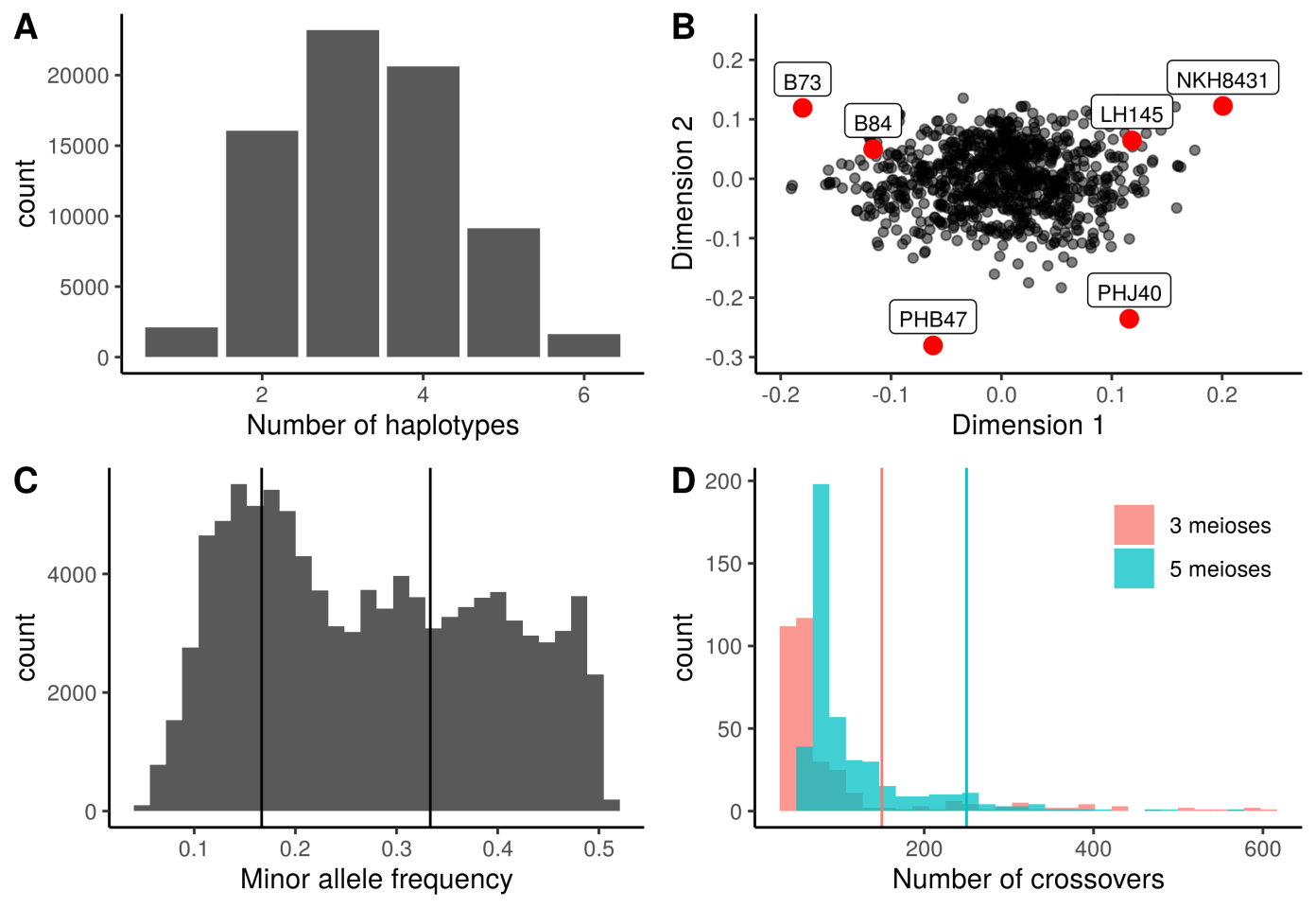
A
count
20000
15000
10000
5000
0
2
4
6
Number of haplotypes
B
Dimension 2
0.2
0.1
0.0
-0.1
-0.2
-0.3
B73
B84
LH145
NKH8431
PHJ40
PHB47
-0.2
-0.1
0.0
0.1
0.2
Dimension 1
C
count
4000
2000
0
0.1
0.2
0.3
0.4
0.5
Minor allele frequency
D
count
200
150
100
50
0
3 meioses
5 meioses
200
400
600
Number of crossovers

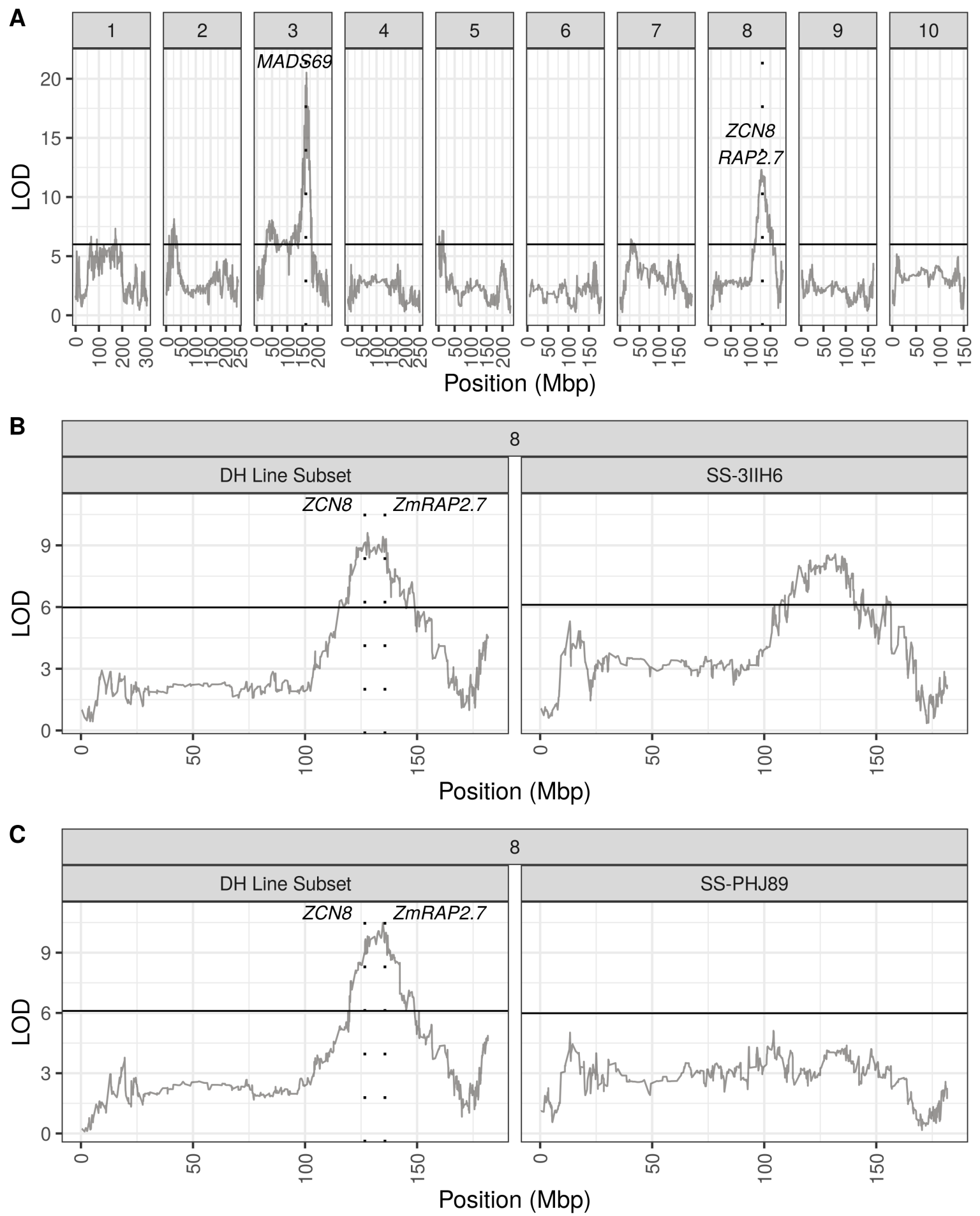
A
1
2
3
4
5
6
7
8
9
10
MADS69
ZCN8
RAP2.7
LOD
Position (Mbp)
B
8
DH Line Subset
SS-3IIH6
ZCN8
ZmRAP2.7
LOD
Position (Mbp)
C
8
DH Line Subset
SS-PHJ89
ZCN8
ZmRAP2.7
LOD
Position (Mbp)

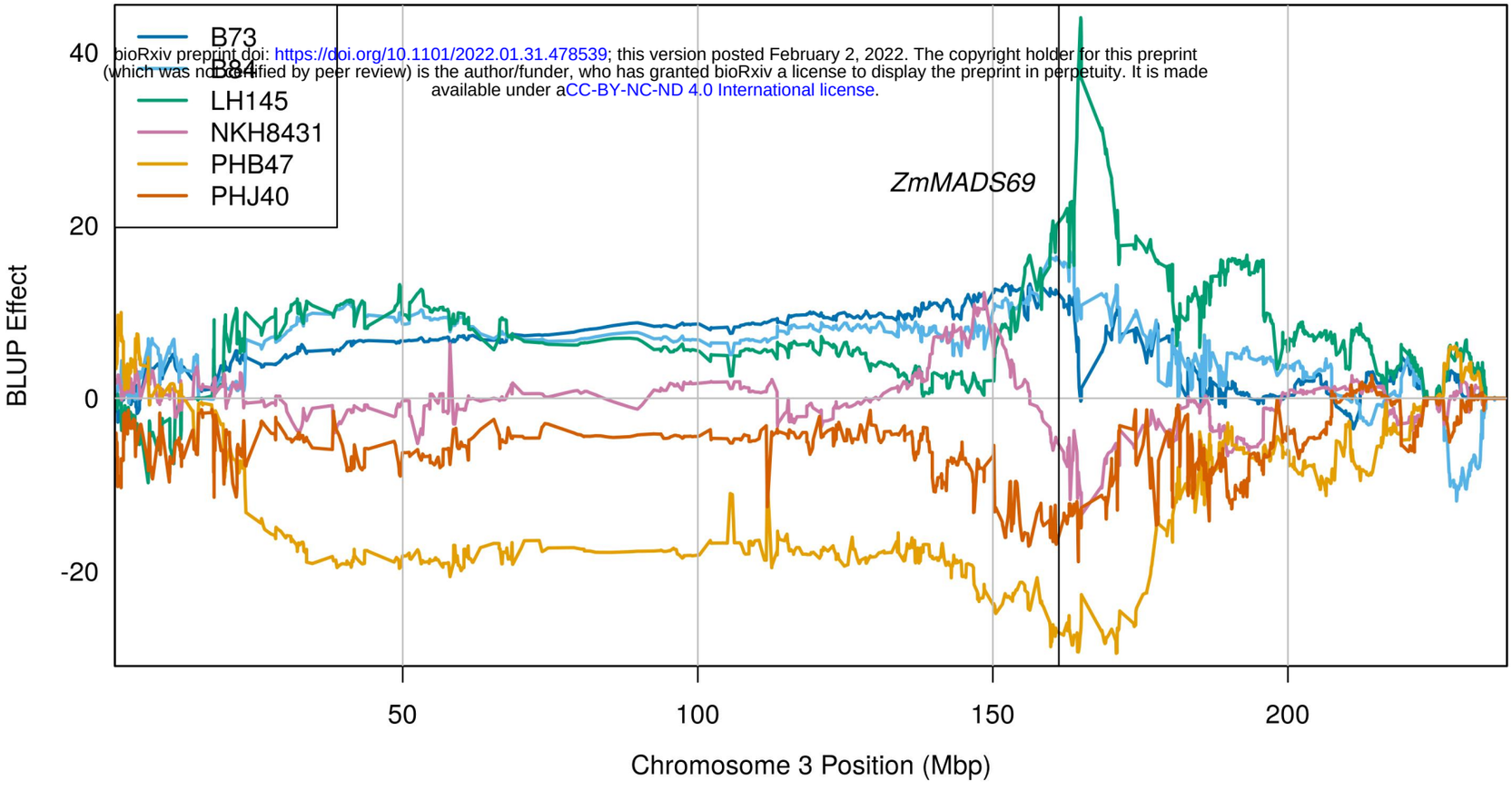

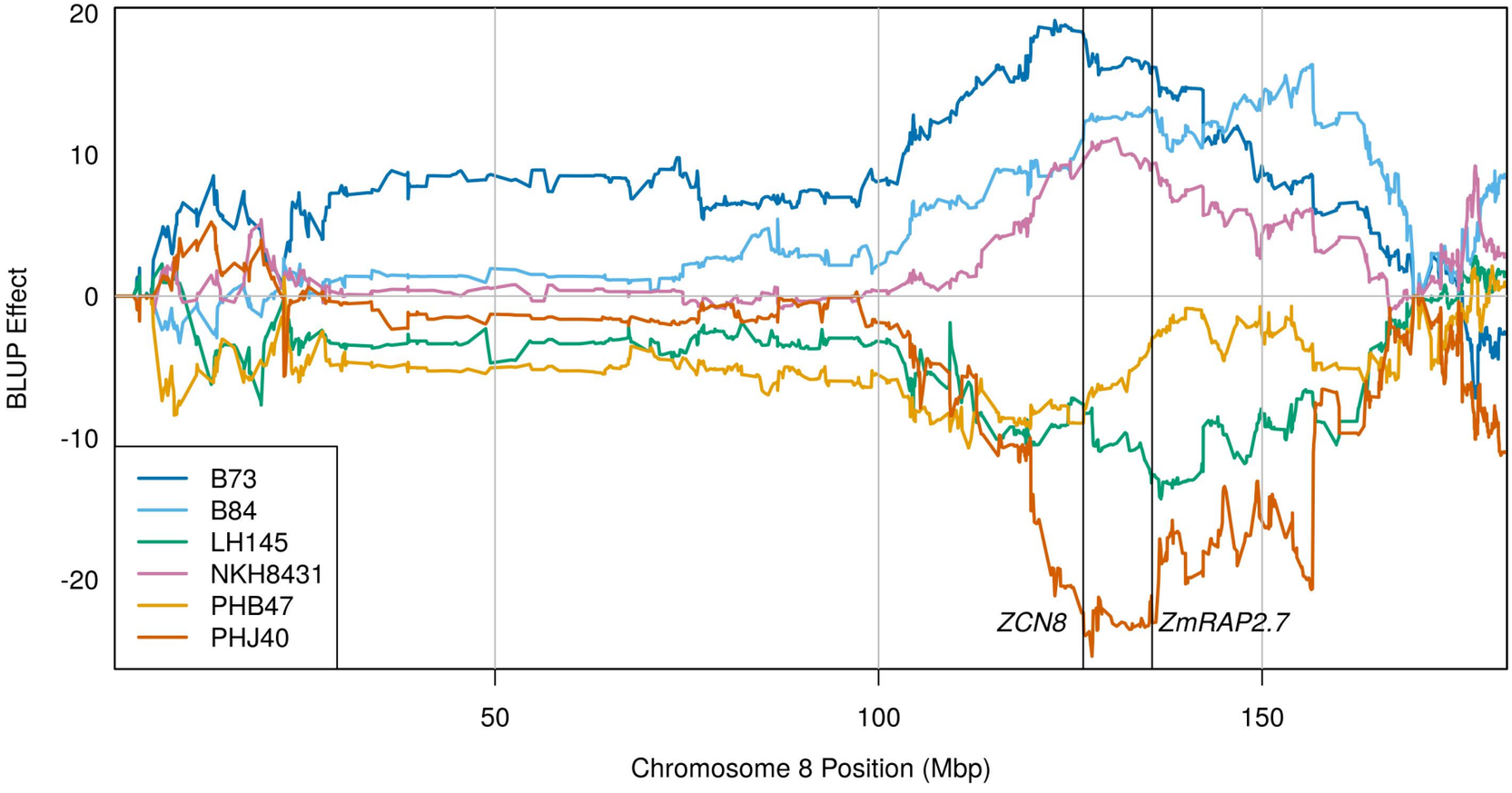

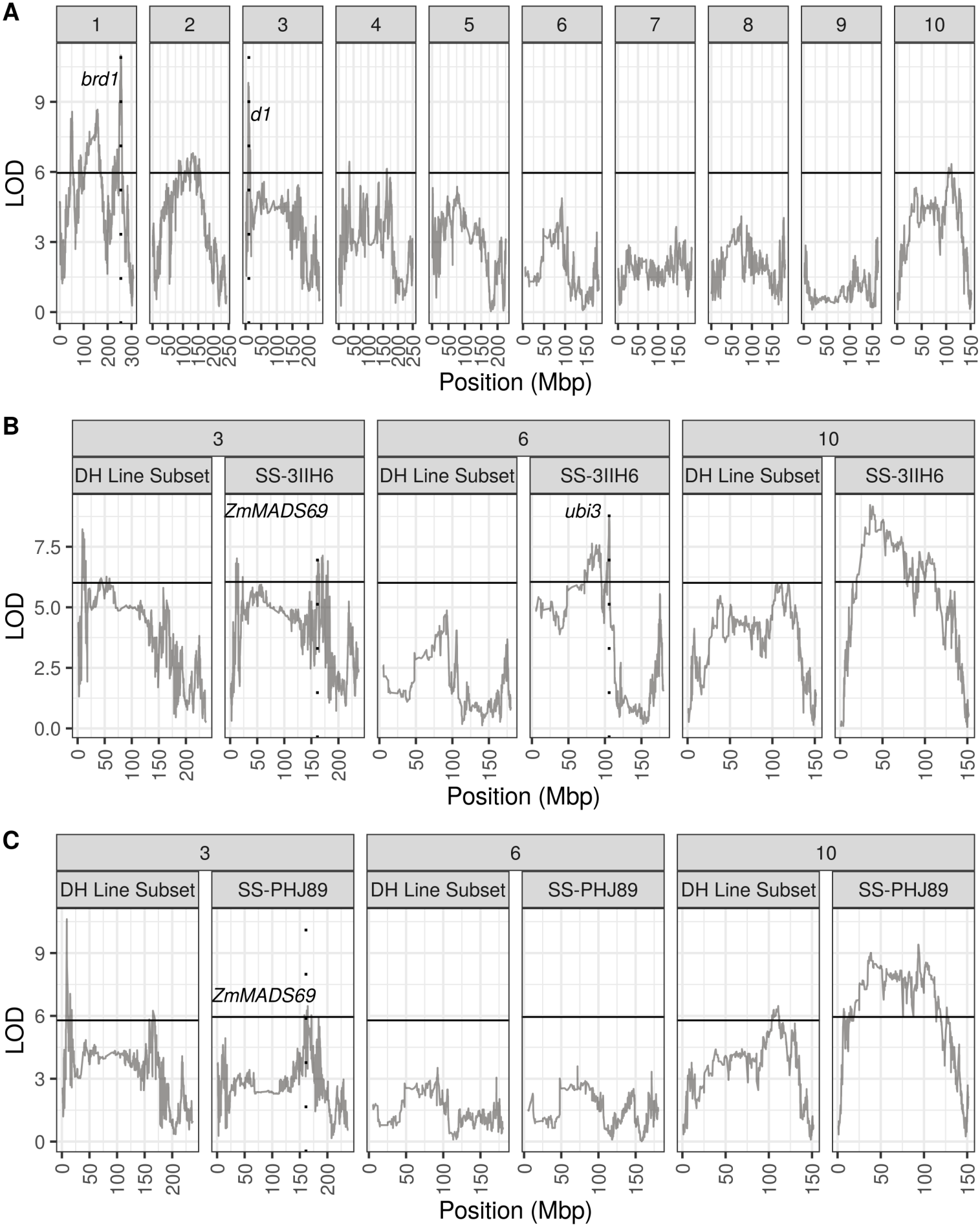
A
1
2
3
4
5
6
7
8
9
10
brd1
d1
LOD
Position (Mbp)
B
3
6
10
DH Line Subset
SS-3IIH6
ZmMADS69
ubi3
LOD
Position (Mbp)
C
3
6
10
DH Line Subset
SS-PHJ89
ZmMADS69
LOD
Position (Mbp)

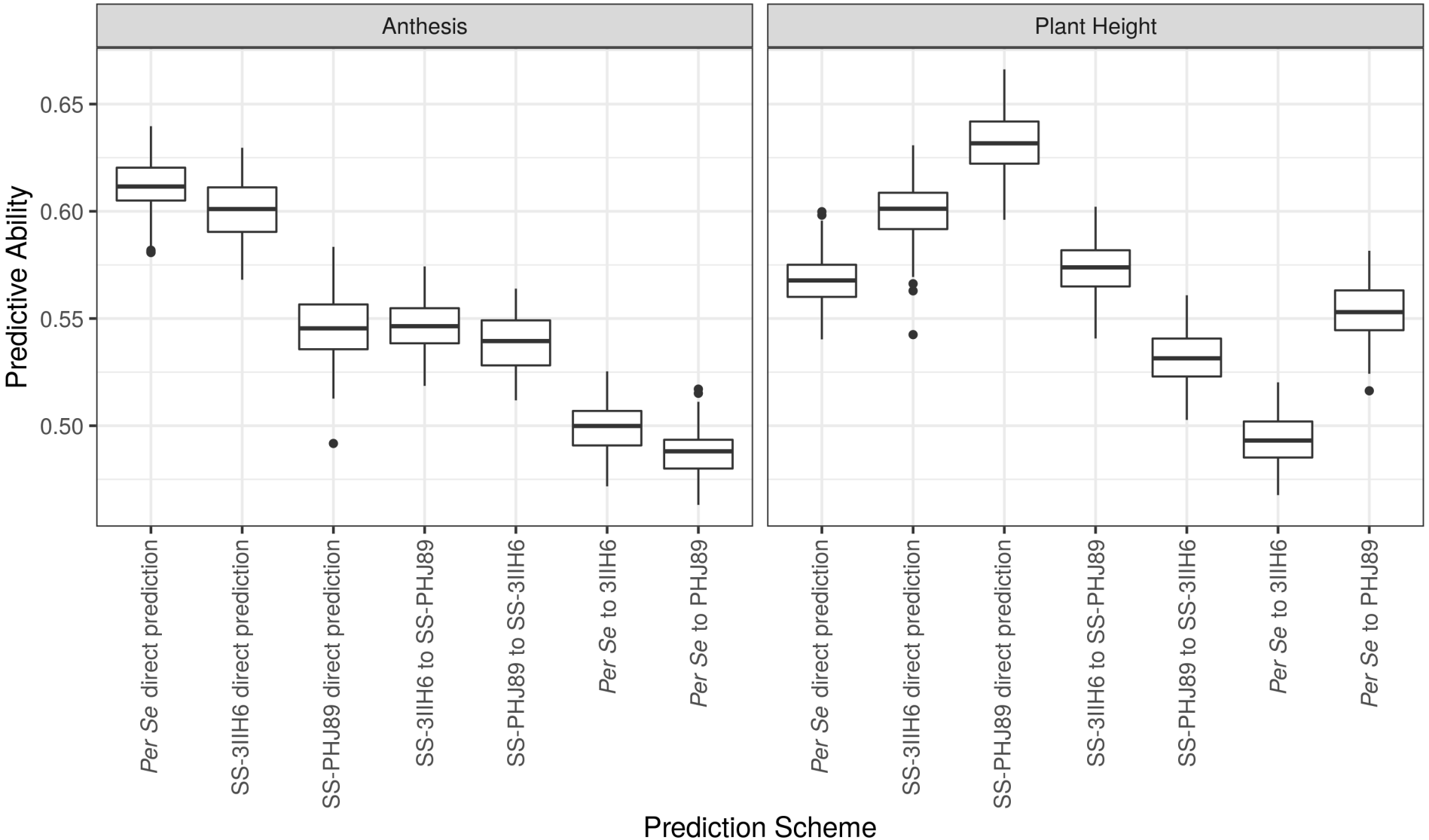
Anthesis
Plant Height
Predictive Ability
0.65
0.60
0.55
0.50
Per Se direct prediction
SS-3IIH6 direct prediction
SS-PHJ89 direct prediction
SS-3IIH6 to SS-PHJ89
SS-PHJ89 to SS-3IIH6
Per Se to 3IIH6
Per Se to PHJ89
Per Se direct prediction
SS-3IIH6 direct prediction
SS-PHJ89 direct prediction
SS-3IIH6 to SS-PHJ89
SS-PHJ89 to SS-3IIH6
Per Se to 3IIH6
Per Se to PHJ89
Prediction Scheme

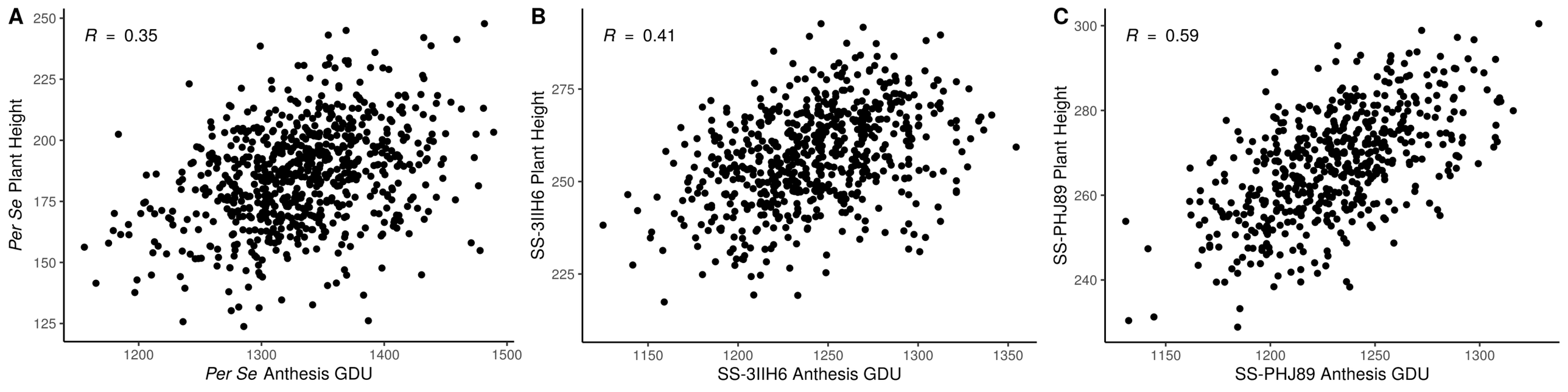
A
R = 0.35
Per Se Plant Height
Per Se Anthesis GDU
250
225
200
175
150
125
1200
1300
1400
1500
B
R = 0.41
SS-3IIH6 Plant Height
SS-3IIH6 Anthesis GDU
275
250
225
1150
1200
1250
1300
1350
C
R = 0.59
SS-PHJ89 Plant Height
SS-PHJ89 Anthesis GDU
300
280
260
240
1150
1200
1250
1300

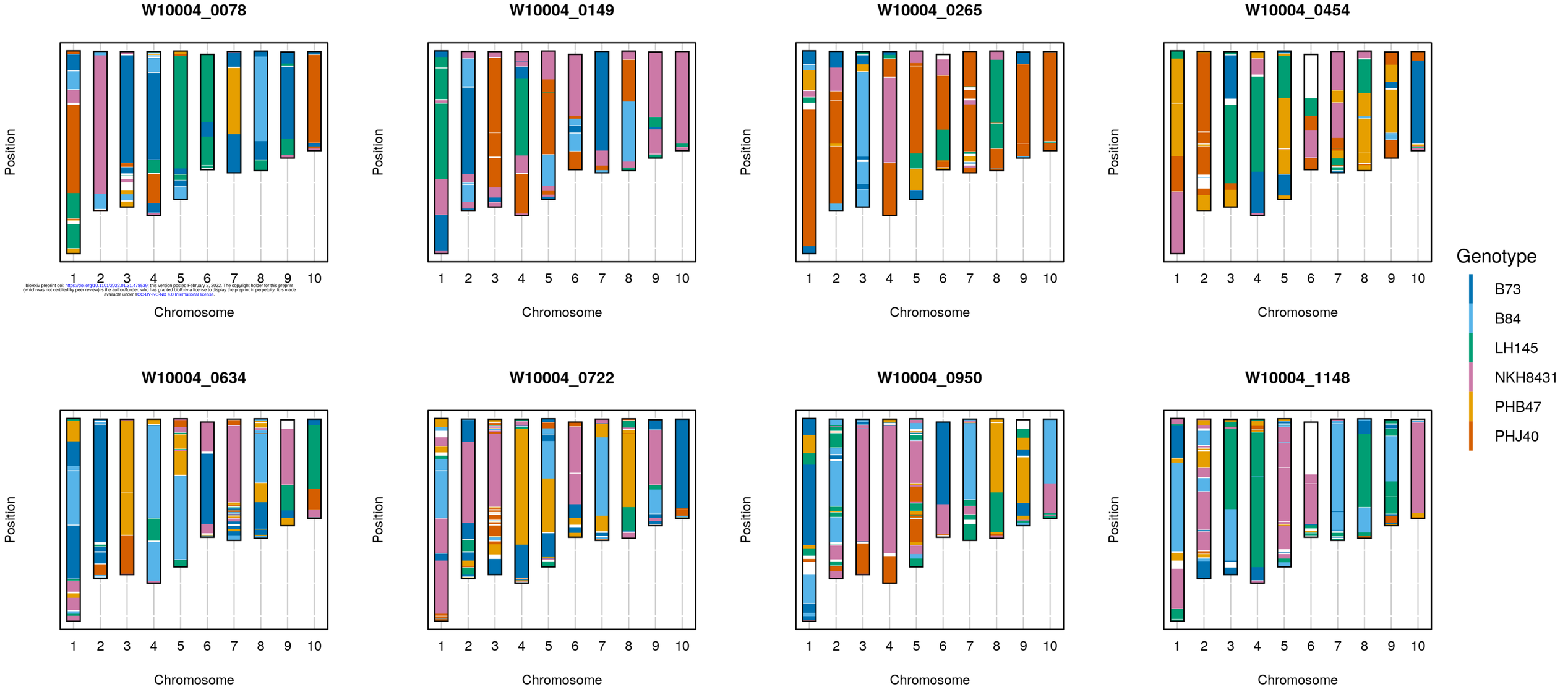

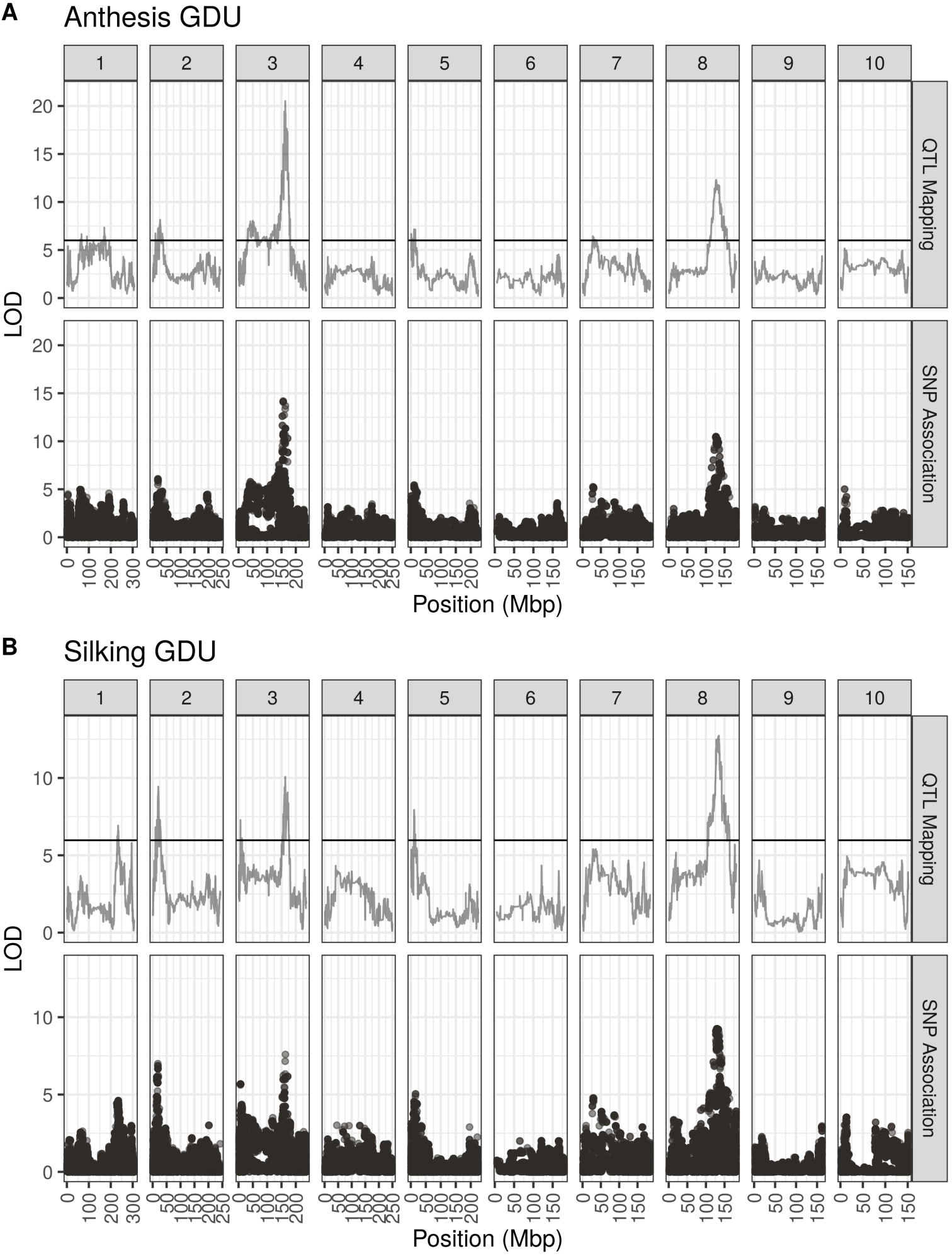
A
Anthesis GDU
1
2
3
4
5
6
7
8
9
10
QTL Mapping
SNP Association
LOD
Position (Mbp)
B
Silking GDU
1
2
3
4
5
6
7
8
9
10
QTL Mapping
SNP Association
LOD
Position (Mbp)

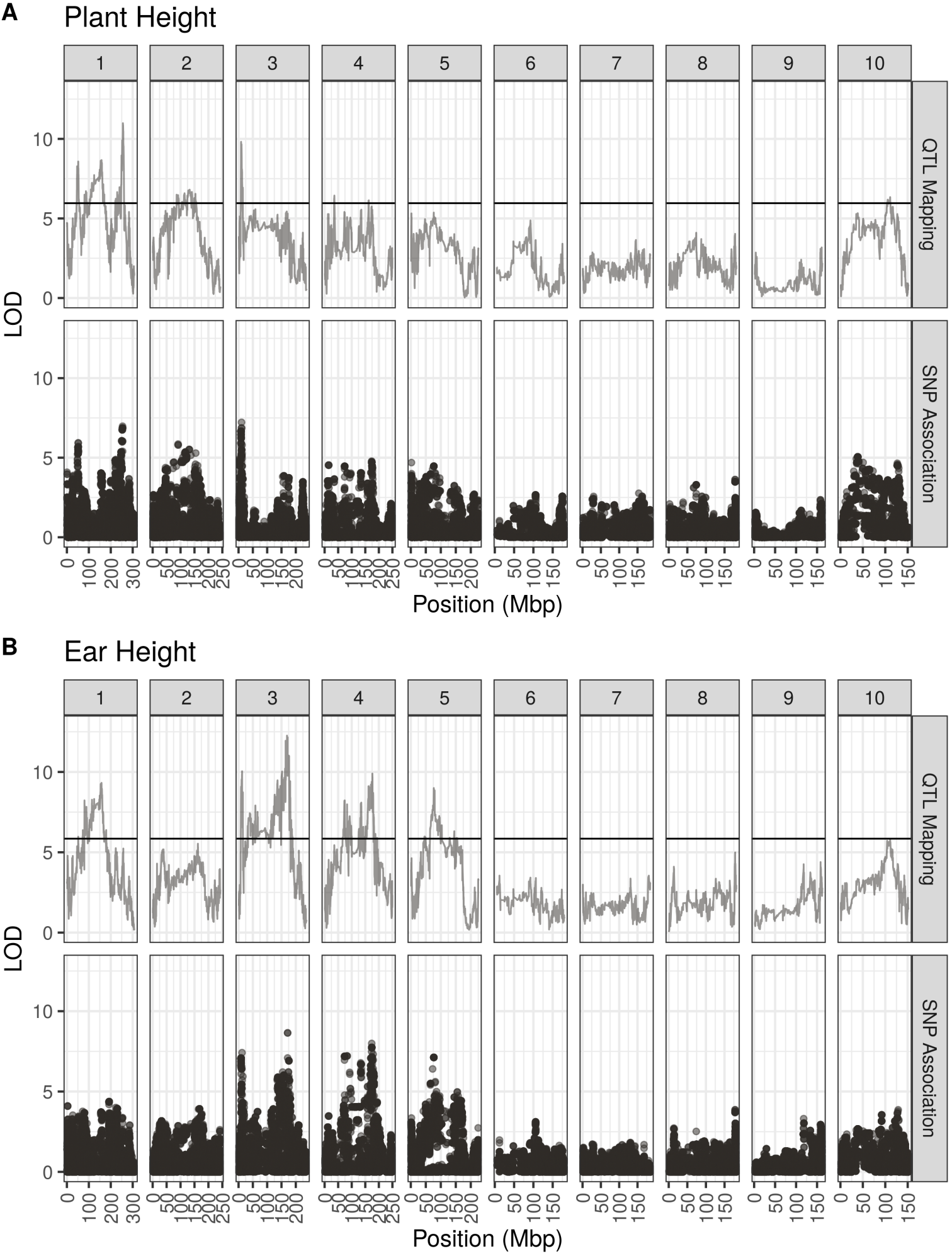
A
Plant Height
1
2
3
4
5
6
7
8
9
10
QTL Mapping
SNP Association
LOD
Position (Mbp)
B
Ear Height
1
2
3
4
5
6
7
8
9
10
QTL Mapping
SNP Association
LOD
Position (Mbp)

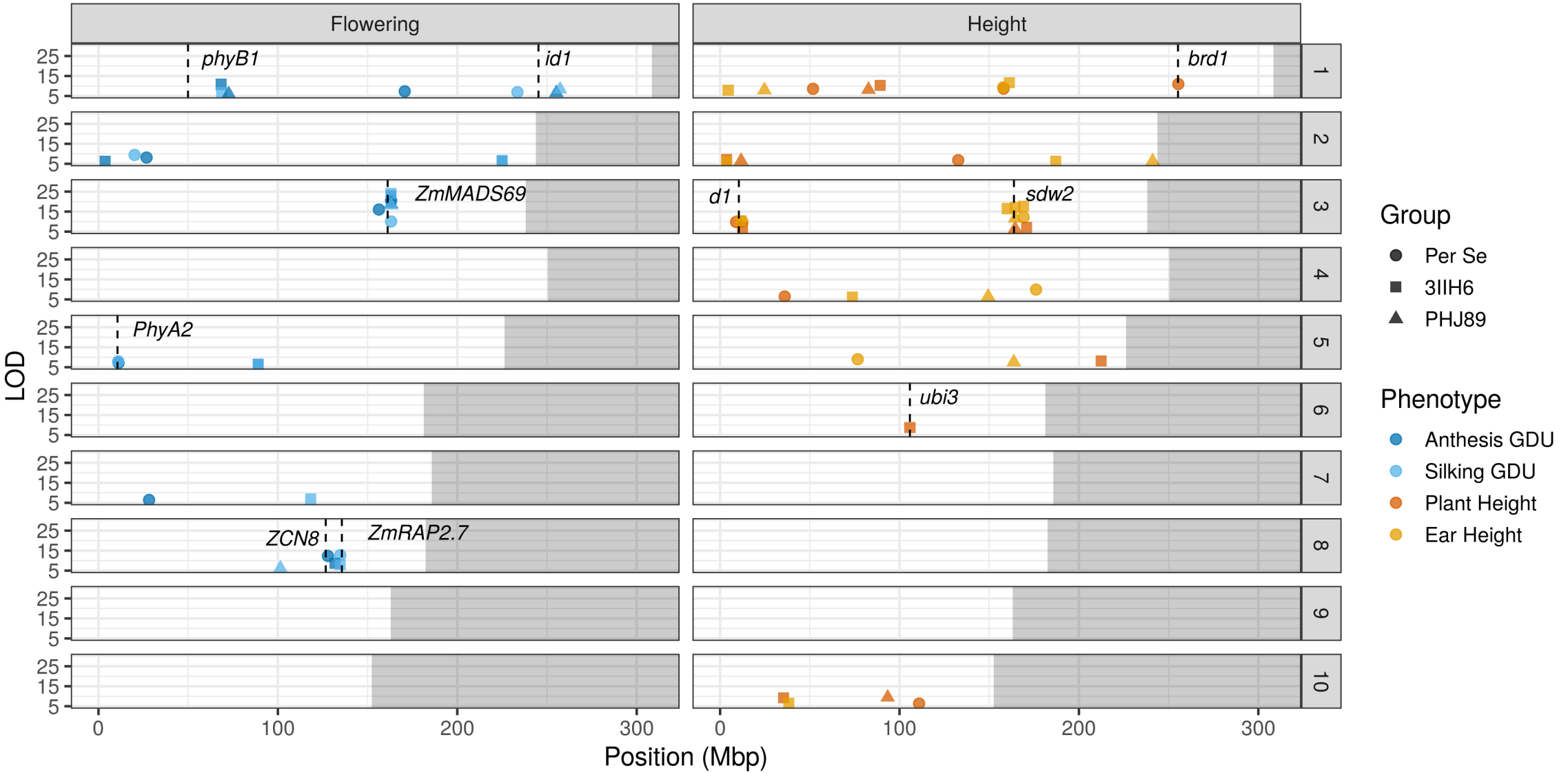
Flowering
Height
phyB1
id1
brd1
ZmMADS69
d1
sdw2
PhyA2
ubi3
ZCN8
ZmRAP2.7
LOD
25
15
5
1
2
3
4
5
6
7
8
9
10
0
100
200
300
Position (Mbp)
Group
Per Se
3IIH6
PHJ89
Phenotype
Anthesis GDU
Silking GDU
Plant Height
Ear Height

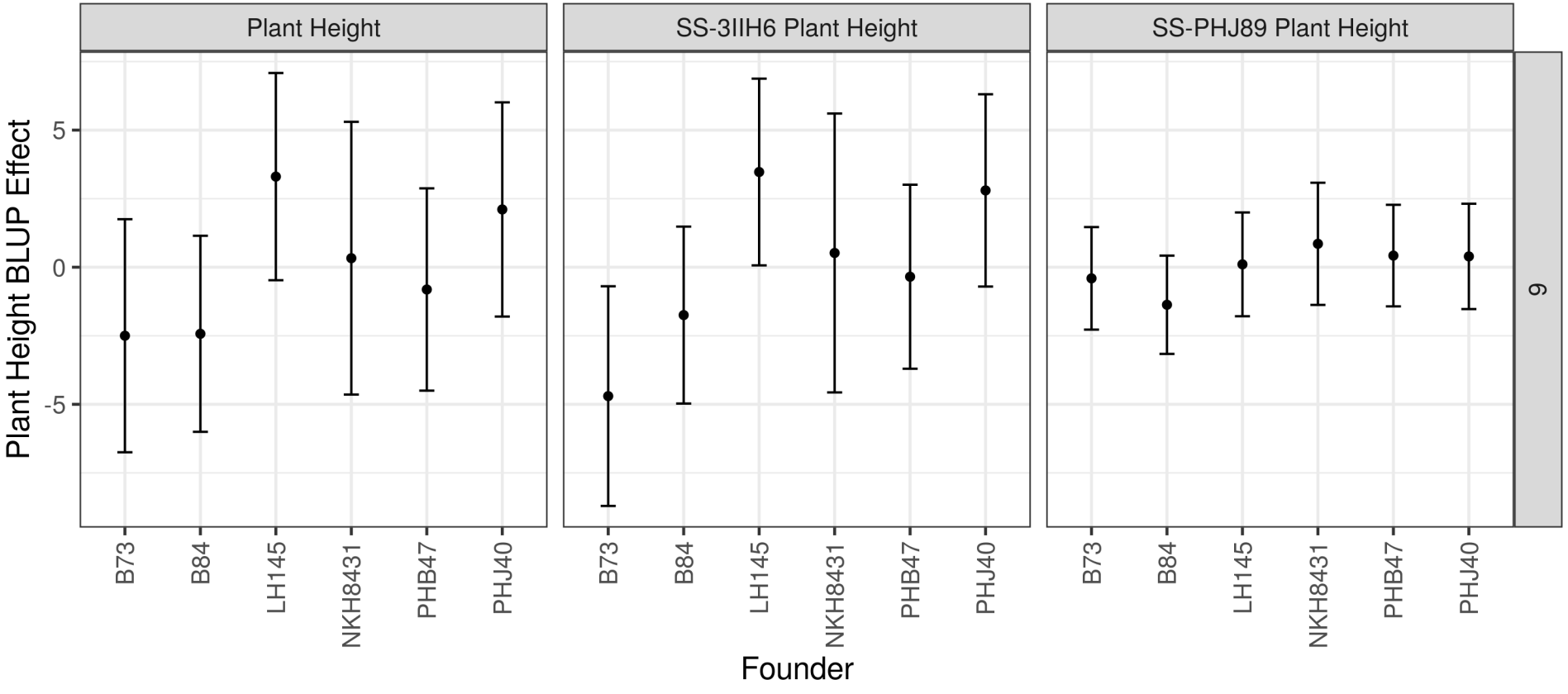
Plant Height
SS-3IIH6 Plant Height
SS-PHJ89 Plant Height
6
Plant Height BLUP Effect
5
0
-5
B73
B84
LH145
NKH8431
PHB47
PHJ40
Founder

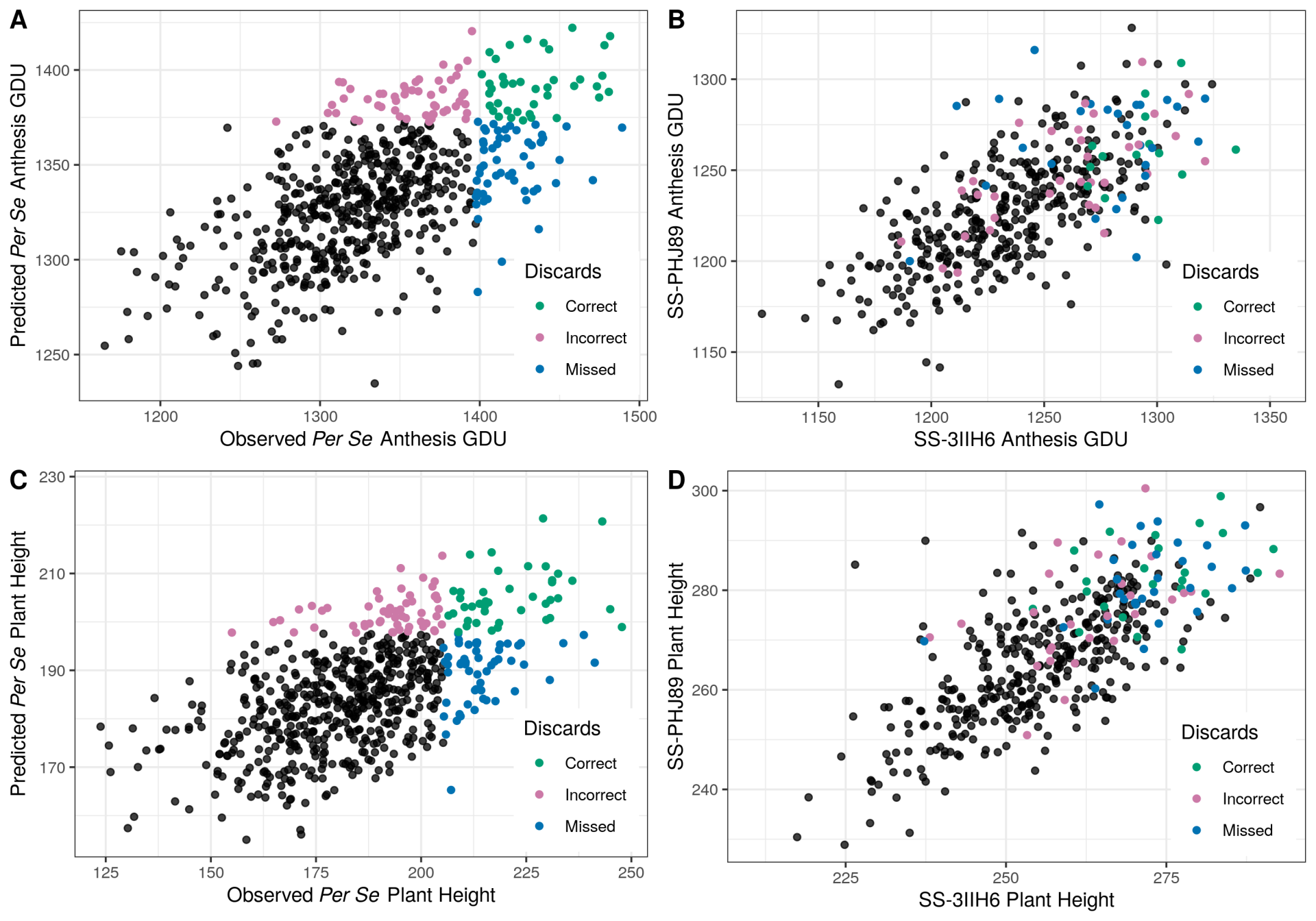
A
Predicted Per Se Anthesis GDU
Observed Per Se Anthesis GDU
1400
1350
1300
1250
1200
1300
1400
1500
Discards
Correct
Incorrect
Missed
B
SS-PHJ89 Anthesis GDU
SS-3IIH6 Anthesis GDU
1300
1250
1200
1150
1150
1200
1250
1300
1350
Discards
Correct
Incorrect
Missed
C
Predicted Per Se Plant Height
Observed Per Se Plant Height
230
210
190
170
125
150
175
200
225
250
Discards
Correct
Incorrect
Missed
D
SS-PHJ89 Plant Height
SS-3IIH6 Plant Height
300
280
260
240
225
250
275
Discards
Correct
Incorrect
Missed

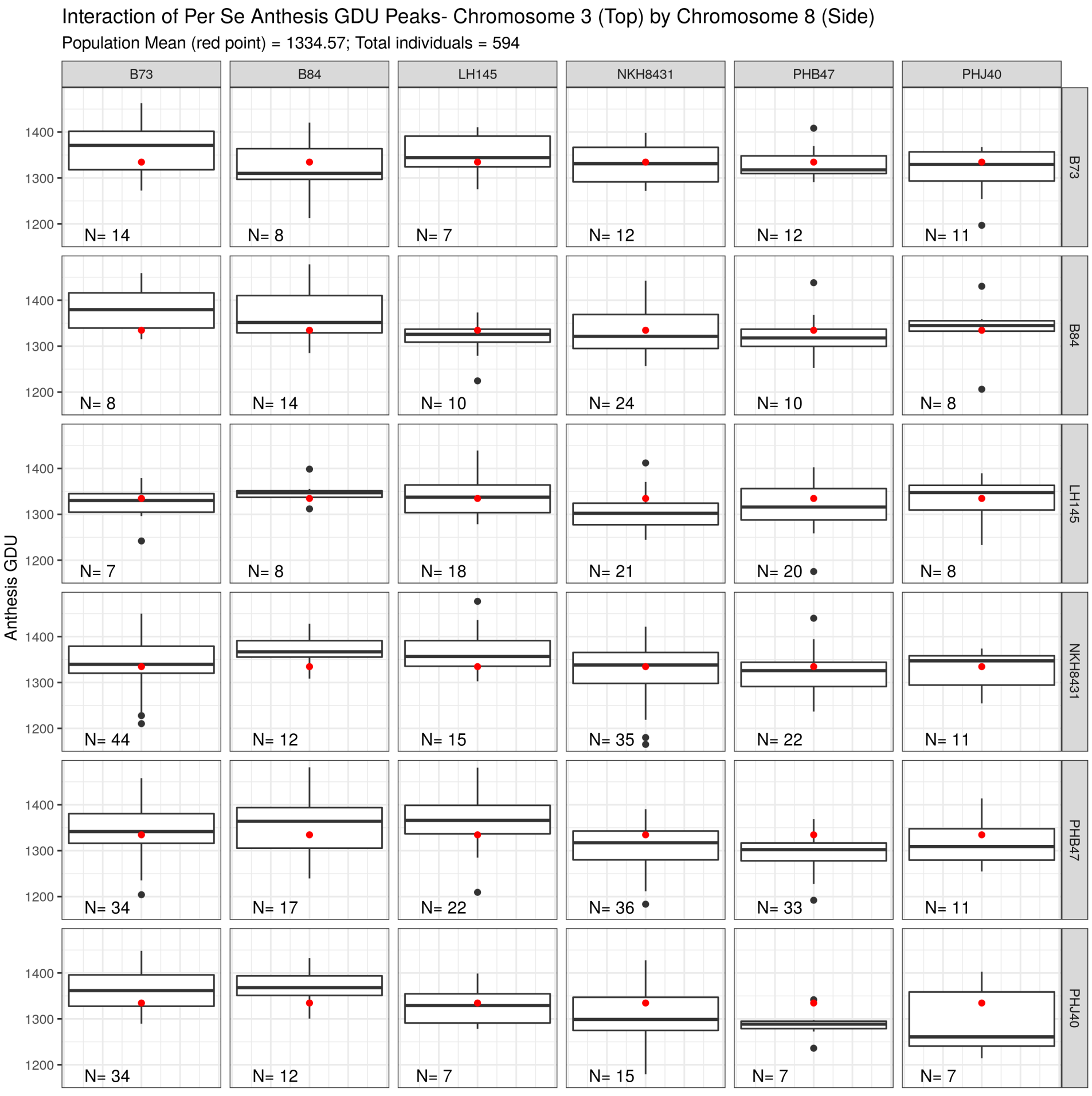
Interaction of Per Se Anthesis GDU Peaks- Chromosome 3 (Top) by Chromosome 8 (Side)
Population Mean (red point) = 1334.57; Total individuals = 594
B73
B84
LH145
NKH8431
PHB47
PHJ40
Anthesis GDU
1400
1300
1200
N= 14
N= 8
N= 7
N= 12
N= 12
N= 11
N= 8
N= 14
N= 10
N= 24
N= 10
N= 8
N= 7
N= 8
N= 18
N= 21
N= 20
N= 8
N= 44
N= 12
N= 15
N= 35
N= 22
N= 11
N= 34
N= 17
N= 22
N= 36
N= 33
N= 11
N= 34
N= 12
N= 7
N= 15
N= 7
N= 7

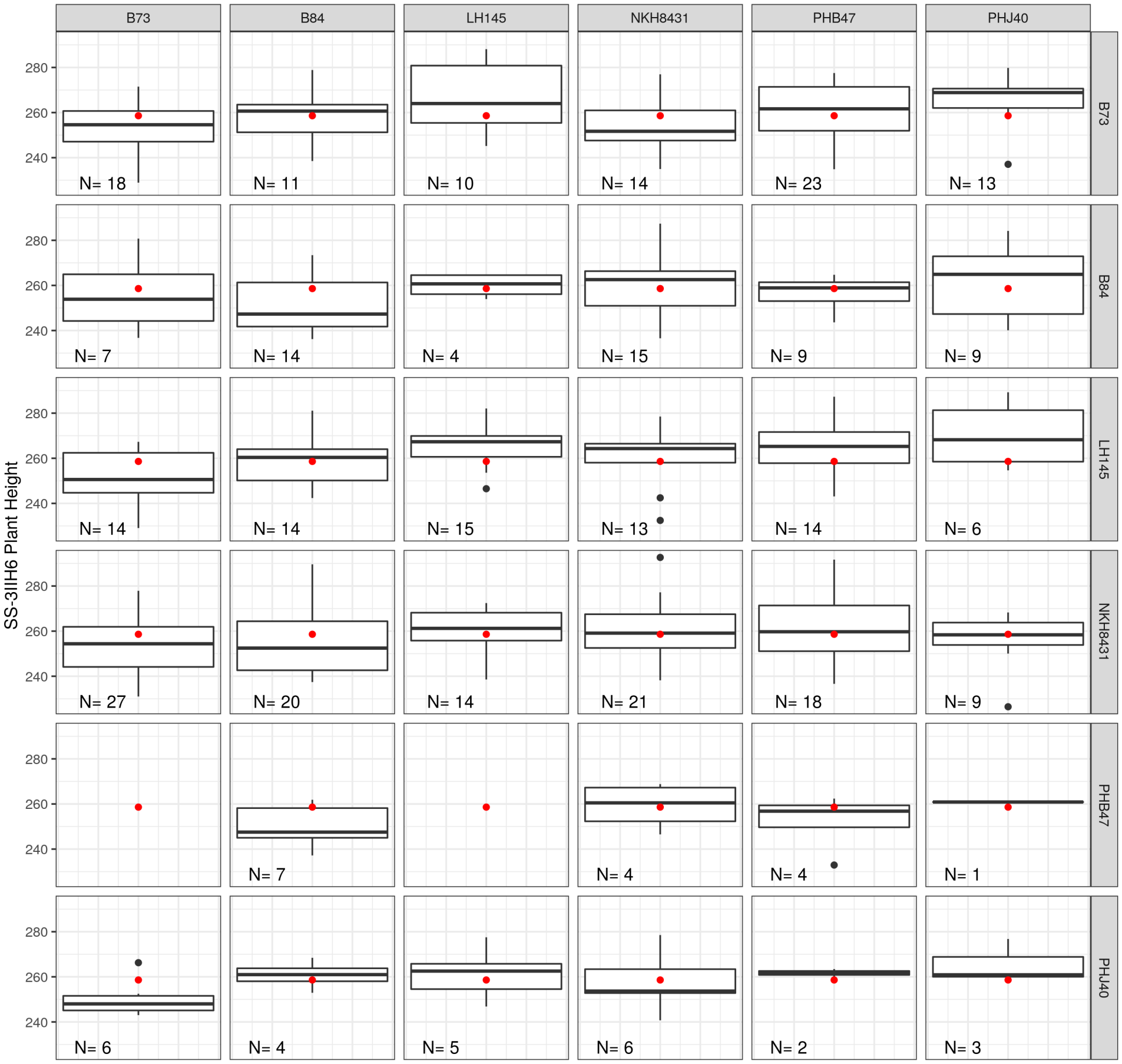
Interaction of SS-3IIH6 Plant Height Peaks- Chromosome 1 (Side) by Chromosome 6 (Top)
Population Mean (red point) = 258.61; Total individuals = 374
B73
B84
LH145
NKH8431
PHB47
PHJ40
SS-3IIH6 Plant Height
280
260
240
N= 18
N= 11
N= 10
N= 14
N= 23
N= 13
N= 7
N= 14
N= 4
N= 15
N= 9
N= 9
N= 14
N= 14
N= 15
N= 13
N= 14
N= 6
N= 27
N= 20
N= 14
N= 21
N= 18
N= 9
N= 7
N= 4
N= 4
N= 1
N= 6
N= 4
N= 5
N= 6
N= 2
N= 3